

Renormalization-group running induced cosmic inflation

I.G. Márián, a N. Defenu, b U.D. Jentschura, c,d,e A. Trombettoni f,g and I. Nándori a,d,e,1

D-69120 Heidelberg, Germany

Via Bonomea 265, I-34136 Trieste, Italy

^gSISSA and INFN — Sezione di Trieste, Via Bonomea 265, I-34136 Trieste, Italy

E-mail: marian.istvan.gabor@science.unideb.hu, ndefenu@phys.ethz.ch, ulj@mst.edu, andreatr@sissa.it, nandori.istvan@science.unideb.hu

Received September 6, 2019 Revised February 14, 2020 Accepted May 6, 2020 Published June 15, 2020

Abstract. As a contribution to a viable candidate for a standard model of cosmology, we here show that pre-inflationary quantum fluctuations can provide a scenario for the long-sought initial conditions for the inflaton field. Our proposal is based on the assumption that at very high energies (higher than the energy scale of inflation) the vacuum-expectation value (VeV) of the field is trapped in a false vacuum and then, due to renormalization-group (RG) running, the potential starts to flatten out toward low energy, eventually tending to a convex one which allows the field to roll down to the true vacuum. We argue that the proposed mechanism should apply to large classes of inflationary potentials with multiple concave regions. Our findings favor a particle physics origin of chaotic, large-field inflationary models as we eliminate the need for large field fluctuations at the GUT scale. In our analysis, we provide a specific example of such an inflationary potential, whose parameters can be tuned to reproduce the existing cosmological data with good accuracy.

Keywords: particle physics - cosmology connection, initial conditions and eternal universe, non-gaussianity, cosmological parameters from CMBR

ArXiv ePrint: 1909.00580

^aUniversity of Debrecen, P.O.Box 105, H-4010 Debrecen, Hungary

 $^{{}^}b {\rm Institut}$ für Theoretische Physik, Universität Heidelberg,

^cDepartment of Physics, Missouri University of Science and Technology, Rolla, Missouri 65409, U.S.A.

^dMTA-DE Particle Physics Research Group, P.O. Box 51, H–4001 Debrecen, Hungary

 $[^]e\mathrm{MTA}$ Atomki, P.O. Box 51, H–4001 Debrecen, Hungary

^fCNR-IOM DEMOCRITOS Simulation Center,

¹Corresponding author.

1	Introduction	1
2	RG and initial condition problem	2
	2.1 Overview	2
	2.2 RG running and inflationary scenarios	3
	2.3 Proposed method	5
	2.4 Suitability of the ϕ^6 and MSG models	5
3	Pre-inflation and slow-roll: analytic and numerical approach	7
	3.1 RG flow of the MSG model	7
	3.2 Pre-inflationary period and RG running	10
	3.3 Inflationary period and slow roll	11
	3.4 Fit to experimental data for small β	13
	3.5 Fit to experimental data for large β	14
4	Conclusions	16
\mathbf{A}	RG running and Hubble time	17
В	Slow-roll studies of alternative models	18
	B.1 Slow-roll study of the MSG model	18
	B.2 Slow-roll study of the ϕ^6 model	24
\mathbf{C}	Convexity and RG running	25
D	RG evolution of the constant term	27

1 Introduction

Contents

Despite the efforts made to construct a standard model of cosmology which explains the exponentially fast expansion [1–5] of the early Universe, important questions remain to be answered. According to current opinion, the hypothetic inflaton field is assumed to slowly roll down from a potential hill towards its minimum. Particle physics provides us with candidates for the inflaton field, where the equation of state required for exponential expansion is modeled by a slowly-moving scalar condensate. Several inflationary scenarios exist (see e.g., ref. [6]). The simplest among these is the quadratic, large field inflationary (LFI) scalar potential, $V(\phi) = \frac{1}{2}m^2\phi^2$.

In fact, the origin and the precise mechanism of inflation is one of the most pressing questions in our understanding of the early Universe after the Big Bang. A first guess would involve a scalar field ϕ (the inflaton field), with an action including the scalar curvature R,

$$S[\phi] = -\int d^4x \sqrt{-g} \left[\frac{1}{2} \nabla_{\mu} \phi \, \nabla^{\mu} \phi + V(\phi) - \frac{m_p^2}{2} R \right], \tag{1.1}$$

where the Planck mass $m_p^2 \equiv 1/(8\pi G)$ has been used and $\sqrt{-g} = \sqrt{-\det g_{\mu\nu}} = a^3$ with $g_{\mu\nu} = \mathrm{diag}(-1, a^2, a^2, a^2)$. Here, the scale factor a = a(t) describes the cosmological scaling

in the Friedmann-Lemaître-Robertson-Walker (FLRW, see refs. [7–10]) metric (in our units, the speed of light is $c \equiv 1$ and $\hbar \equiv 1$).

It is commonly assumed that thermal fluctuations of cosmic microwave background radiation (CMBR) originated from quantum fluctuations of the background (the inflaton field and the metric) during the inflationary period. Thus, details of the self-interaction potential of the inflaton influence thermal fluctuations of the CMBR, and can be confronted with Planck data [11–13], which measures thermal fluctuations of the background radiation. Of course, a reliable model should provide agreement with observations. For example, the quadratic LFI model is almost excluded by recent results of the Planck mission [11–13]. By the slow-roll analysis, one can decide whether a particular choice for an inflationary potential can serve as a viable model, i.e., whether it agrees with Planck data.

Following refs. [4, 5], one can use a modification of the original idea of Alan Guth [1], where the ground state starts from a metastable position and then, somewhat surprisingly, rolls down very slowly to the true minimum. This scenario, as is well known, solves a number of problems connected with the original idea formulated in the seminal paper [1]. Yet, concerning the slow-roll scenario, one may ask why the inflaton field should start from a particular, well-defined slow-roll domain (this is commonly referred to as the "initial condition problem").

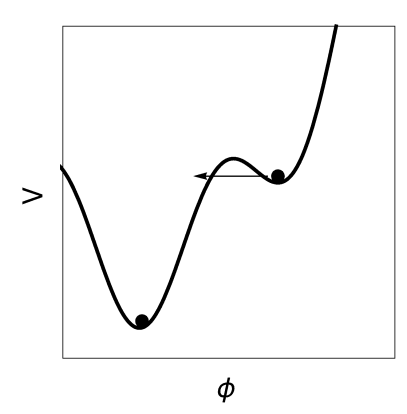
This paper is centered around the mentioned questions and is organized as follows. We provide an initial account of the interrelation of the renormalization-group (RG) which we propose for a description of the pre-inflationary period, and the slow-roll mechanism during inflation (see section 2). Details include remarks on the method of analysis proposed by us (section 2.3) and the suitability of the ϕ^6 versus the massive sine-Gordon (MSG) models (section 2.4). We proceed to both a numerical as well as an analytic approach to the required RG flow equations, and their relation to the slow-roll of the potential (section 3). Conclusions are reserved for section 4. Four appendices supplement the considerations. One is for details on the relation between RG running and Hubble time (appendix A), another one is concerned with the dependence of the slow-roll analysis on the particular choice of the model (appendix B). Two more appendices deal with general considerations regarding convexity of the potential and RG running (appendix C), and with the RG evolution of the field-independent, constant term $V_k(0)$ (appendix D).

2 RG and initial condition problem

2.1 Overview

The original idea of Alan Guth for inflation is based on the existence of a relatively stable false vacuum which can be long-lived or metastable (see ref. [1]). The system moves to the true vacuum through a bubble nucleation caused by instanton effects via quantum tunneling; this induces inflation. A larger energy difference between the two vacua and, alternatively, a smaller height or width of the barrier increases the tunneling rate. Inside bubbles, the field has its true vacuum value, and these regions of space have lower energy, so when bubbles are nucleated, they begin to expand at nearly the speed of light. However, this old scenario for inflation (see figure 1) suffers from problems.

For example, it is required to heat up the Universe after the inflation period and it is not clear how to define a proper reheating mechanism. In order to produce the present observable Universe, exponential expansion should continue long enough to eliminate magnetic monopoles, but then bubbles become very rare and in addition, they never merge. This



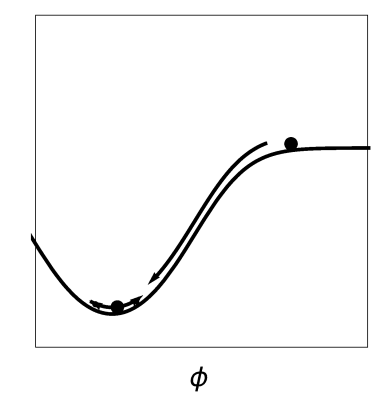


Figure 1. Inflation from false vacuum (left) and by slow-roll (right) where oscillations of the field produce reheating.

generates two major problems: (i) the decay process is never complete, (ii) radiation cannot be generated by collisions between bubble walls (which was the proposed mechanism for radiation).

A possible solution for problems of bubble nucleations is provided by a scenario proposed in refs. [4, 5], where the ground state starts from a metastable position and rolls down very slowly to the true minimum (see figure 1). Thus, inflation is thought to be caused by a scalar field rolling down a potential energy hill instead of tunneling out of a false vacuum. The inflation is over when the hill becomes steeper. This, in particular, solves the problem of formulating a "graceful exit" from the inflation period.

This leaves the initial condition problem to be addressed. Chaotic (large-field) inflation [14] can resolve this issue since it is natural to assume large field values at the energy scale of inflation, but then, as a consequence, quantum fluctuations dominate over the classical evolution of the inflaton field providing regions where the field moves up the potential. This could result in eternal inflation, leading to a multiverse and the theory could loose its predictive power. Initial conditions are even more problematic for small-field inflation where interactions have to homogenize the Universe on a scale larger than the horizon. Models other than cosmic inflation, like the theory of the cyclic Universe [15, 16], have also been discussed in order to overcome the problem of eternal inflation.

Moreover, the shape of the inflaton potential is not known except that it must be sufficiently flat for the slow-roll mechanism. Therefore, the proper treatment of quantum fluctuations is important; this may require renormalization and, in turn, may result in scaling (running) parameters modifying the potential itself. Indeed, the use of renormalization-group (RG) techniques is a standard choice in the post-inflation period within Higgs-particle-induced inflation models (for a recent overview, see ref. [17]).

2.2 RG running and inflationary scenarios

Pursuant to the suggested relevance of RG running for the description of inflation, our main goal here is to discuss a mechanism which could connect the original (ref. [1]) and the modern (refs. [4, 5]) scenarios for inflation, or, more precisely, to investigate how the renormalization-group (RG) running of the inflationary potential could imply a possible solution for the initial condition problem.

During inflation itself, the slow roll-down of the VeV is commonly considered as a classical process. However, our focus here is on the pre-inflationary period, where RG running is widely used [18-27]. Indeed, a series of papers are discussing the RG evolution of the Einstein equation or, more generally, Quantum Einstein Gravity and the Friedmann-Lamaître-Robertson-Walker (FLRW) cosmology [28–30] by using the ideas of refs. [18–27], where the running momentum scale k of the RG approach is identified with the inverse of the cosmological time $(k \sim 1/t)$. The identification of cosmological time evolution with RG running has been advocated, quite recently, in a series of papers [24, 27, 50–54], with a particular focus on the cosmological constant, which has been parameterized in terms of the density $\rho = \Lambda/(8\pi G)$ [see the text before eq. (1) of ref. [54], eq. (3) of ref. [54], and eq. (10) of ref. [53]]. The model has been termed the "running vacuum model" (RVM). In our model (see also appendix D), the cosmological constant term appears as the field-independent term, for which we observe a perfect analogy of our RG equation (D.1) with eq. (3) of [54] and eq. (10) of ref. [53], upon the identification $H \sim k$. This observation further supports our working hypothesis [18-27] that $H \sim k$ can be identified with the inverse of the cosmological time parameter. The RVM (see refs. [24, 27, 50–54]) is an extension of the ΛCDM model (cosmological constant cold dark matter model) via a dynamical vacuum energy density. Our work supports this hypothesis, and it is consistent with the recent work [54] where the RG running is found to be consistent with results derived from the bosonic (inflaton+axion) sector of an effective action which is adjusted so that it reproduces the string scattering amplitudes to lowest nontrivial order in an expansion in the string Regge slope [see eq. (14)] of ref. [54]]. While in this paper, the identification of the RG running scale k and the Hubble parameter is heuristically assumed, we stress, as already outlined, that this approach can be demonstrated from first principles by relating the effective field theory under consideration with the string theory action which results in the Cosmological "Running Vacuum" type model for the Universe, see [24, 27, 50–52]. For further details see appendix A.

In our RG-inspired model, the VeV is assumed to be trapped in a false vacuum in the preinflationary period at very high energies, and then, due to quantum fluctuations, as described by the RG, the effective potential is modified releasing the VeV and leading to the classical inflationary evolution at the scale of inflation. Note that the RG evolution of the (selfinteraction) potential of the inflaton field is a consequence of its own scale-dependent quantum fluctuations; the above scenario welcomes the existence of further quantum fluctuations below the scale of inflation, where the slow-roll process is otherwise considered to be "classical". However, the quantum fluctuations below the scale of inflation are of less importance because the false vacuum has already disappeared.

The main idea behind our proposed method for RG running induced inflation is the fact that any scalar potential should tend to a convex one during the RG flow. We show that the RG evolution of the potential starts from a concave potential at high energies, (i.e., at the Planck scale) which ensures that the VeV can be trapped; it tends to a less concave one at lower energies (i.e. at the GUT scale) and releases the VeV to initiate inflation. RG running is expected to provide a sufficient change in the shape of the potential between the two scales. Let us note that we show this general picture by explicit calculations with RG equations obtained in flat Euclidean space. One might argue that, nevertheless, a more reliable RG study can take into account for example the corresponding curved spacetime effects. Indeed, functional RG in an FLRW metric space has been discussed, for instance, in [31–34]. The field is assumed to propagate in above mentioned FLRW cosmological background with the metric, $ds^2 = a^2(\tau) \left[-d\tau^2 + d\vec{x}^2 \right]$ (see also appendix A), where τ is the conformal time and

 \vec{x} denotes the comoving spatial coordinates [see eq. (1) of ref. [31]]. The action is defined as [see eq. (2) of refs. [32, 33]]

$$S[\phi] = -\int d^4x \sqrt{-\det g} \left[\frac{1}{2} \nabla_{\mu} \phi \, \nabla^{\mu} \phi + V(\phi) \right]. \tag{2.1}$$

where $\nabla_{\mu}\phi \nabla^{\mu}\phi = \sum_{\mu=1}^{4} (\partial\phi/\partial x_{\mu})^2$ in the sense of a four-dimensional, flat Euclidean space. In comparison to eq. (1.1) above, one drops the term $\frac{1}{2} m_p^2 R$. An inspection of figure 9 of ref. [34] reveals that RG running in the FLRW metric leads to an enhanced convexification with respect to the flat-space approximation used below in eq. (2.5). Since convexification is an essential ingredient of our arguments, the proposed scenario should directly apply also to the non-flat metric calculations. We identify the covariant derivative as ∇^{μ} in eq. (2.1).

2.3 Proposed method

Let us emphasize that the proposed RG-induced mechanism should work for any (differentiable) inflationary potential which (i) has a concave region and (ii) has at least one false vacuum. If these two conditions are fulfilled by the model, one can apply the method in three steps:

- One has to perform the slow-roll study of the model; this puts constraints on the shape of the potential. As a result, the "slow-roll potential" becomes (almost) flat in its concave region where the false vacuum originates, and so, the VeV can roll down slowly over inflation.
- One has to determine the RG running of the potential, i.e. the RG running of the couplings. To generate the RG equations for the couplings a possible choice is to expand the potential into Taylor-series, i.e.,

$$V = V_0 + g_1 \phi + \frac{1}{2!} g_2 \phi^2 + \frac{1}{3!} g_3 \phi^3 + \dots,$$
 (2.2)

which generates the couplings g_1, g_2, g_3, \ldots specific to the particular model. One may expect that, given the existence of a suitable non-perturbatively renormalizable UV completion, the Taylor expansion is a valid method for analyzing the RG flow if an appropriate number of couplings are included.

• Once the RG running of the couplings is determined, one has to choose a model at the Planck scale, so that when it is evolved down to the cosmological scale ($k \sim 10^{16}\,\mathrm{GeV}$), it becomes identical to the slow-roll potential.

2.4 Suitability of the ϕ^6 and MSG models

The simplest model which fulfills the above three conditions and has a \mathbb{Z}_2 symmetry is the scalar potential

$$V_{\phi^6} = \frac{1}{2}g_2\phi^2 + \frac{1}{4!}g_4\phi^4 + \frac{1}{6!}g_6\phi^6, \qquad (2.3)$$

with $g_2 > 0$, $g_4 < 0$ and $g_6 > 0$. It has two false vacua and is here proved to tend to a convex one in the low-energy limit (see appendix C). The VeV is assumed to be trapped in (the only) false vacuum of the ϕ^6 model at very high energies. Near the end of inflation, the parameters of the model can be determined by comparison to PLANCK data (see the

discussion in section 3.4), and the VeV rolls down slowly (see appendix B.2). However, the ϕ^6 model, due to its nonrenormalizability, cannot serve as a viable UV completion of the inflaton potential. and therefore, we here consider the massive sine-Gordon (MSG) model as its simplest renormalizable UV completion (in four dimensions).

Let us first mention that according to refs. [11–13], one finds a certain disagreement of the natural inflation potential [59–61] with Planck results, but the natural (i.e., periodic) inflation model still provides better agreement than the simplest quadratic LFI potential. However, the combination of a polynomial in the field, and additional periodic terms, provides for an attractive alternative scenario. For example, in refs. [62, 63], a linear term is added to the periodic one and proposed as a viable inflationary potential and denoted as an axion monodromy. The linear term implies that the potential is not bounded from below.

Here, our goal is to extend the periodic potential in such a way that: (i) the potential has definite lower bounds, (ii) the model has Z_2 symmetry, and (iii) the model has more than one non-degenerate minima, separated in energy by a tunable amount. The model represents a (nonperturbatively) renormalizable UV completion of the ϕ^6 model with non-degenerate minima. The potential of the massive sine-Gordon (MSG) model, which fulfills these requirements, reads as

$$V_{\text{MSG}}(\phi) = \frac{1}{2}m^2\phi^2 + u\left[1 - \cos(\beta\phi)\right]. \tag{2.4}$$

The full (Euclidean) action S of our theory is local, and is given by

$$S = \int d^4x \left[\frac{1}{2} (\partial_\mu \phi)^2 + V_{\text{MSG}}(\phi) \right], \qquad (2.5)$$

where in comparison to eqs. (1.1) and (2.1), we work in flat space. In order to better understand the connection to the FLRW metric which enters eq. (1.1), let us observe that in a metric of the form

$$g_{\mu\nu} = \text{diag}(-1, a(t)^2, a(t)^2, a(t)^2),$$
 (2.6)

$$ds^2 = -dt^2 + a(t) \, d\vec{r}^2 \,, \tag{2.7}$$

with $\vec{r} = (x, y, z)$, one can replace, in the action in eq. (2.1),

$$\nabla^{\mu}\phi\nabla_{\mu}\phi \to g^{\mu\nu}\partial_{\mu}\phi\partial_{\nu}\phi \to = -\left(\frac{\partial\phi}{\partial t}\right)^{2} + \frac{1}{a(t)^{2}}\left(\frac{\partial\phi}{\partial\vec{r}}\right)^{2}.$$
 (2.8)

One may stretch the spatial coordinates according to

$$\vec{r}' = a(t)\vec{r}, \qquad \phi(t, \vec{r}) = \phi'(t, \vec{r}') \tag{2.9}$$

and re-identify the primed coordinates and fields with the unprimed ones. (The Jacobian of the transformation to the primed coordinates eliminates $\sqrt{-\det g} = a^3$ from the action.) A subsequent Legendre transformation then leads to the Euclidean action given in eq. (2.5), which we use for our RG analysis. We should also clarify that, for the considerations reported below, the scaling (2.9) does not matter as it does not affect the later identification of the running scale k of our RG with a quantity that is a inversely related to a cosmological time parameter, which is all that is required (see also appendix A).

While we focus on the MSG model in the conventions of eq. (2.4), we anticipate that important conclusions of our studies for more general functional forms (see appendix B).

The MSG model contains two adjustable parameters (the ratio u/m^2 and the frequency β) in addition to the usual normalization factor which can be fixed at the cosmological scale by the standard slow-roll analysis. Furthermore, we show in appendix B that an additional constant term does not modify the slow-roll results.

3 Pre-inflation and slow-roll: analytic and numerical approach

3.1 RG flow of the MSG model

If one would like to consider the RG evolution of the parameters of a field theory (e.g. the inflationary potential discussed in the previous section), then a natural choice is the momentum shell (functional RG) method which is based on the RG flow equation [64, 65]. Furthermore, one can try to connect the running momentum scale of the RG method (k) to the cosmological time (t) as it has been done in many papers based on ideas presented in [18–27]. In general, it is not that straightforward to consider time-dependence of a quantum field theory. One has to involve some extension of the theoretical framework such as the closed-time-path (or Schwinger-Keldysh) formalism [66–72] which immediately leads to open quantum systems where typically an external heat bath has to be introduced.

In addition, one can assume the presence of an external bath of particles whose energy might redshift, providing a time-dependent background; this might induce some time dependence which has been used in [73] to solve the so-called overshoot problem. We would like to re-emphasize that we do not follow any of the above attempts and do not assume that RG, eo ipso, necessarily induces a time-dependence. However, it is still permissible to associate the running momentum scale with the cosmological time, as described in detail in appendix A. In general, the (functional) RG allows to treat the effects of quantum fluctuations studying the scale dependence of a model via a blocking construction, and the successive elimination of the degrees of freedom which lie above a running momentum cutoff. This procedure generates the momentum-shell RG (functional RG) flow equation [64, 65] and widely discussed in refs. [74, 75]. In the local potential approximation (LPA) using the Litim regulator [76], this equation is written as

$$\left(d - \frac{d-2}{2}\tilde{\phi}\,\partial_{\tilde{\phi}} + k\partial_k\right)\tilde{V}_k = \frac{2\alpha_d}{d}\,\frac{1}{1 + \partial_{\tilde{\phi}}^2\tilde{V}_k}\,,$$
(3.1)

where $\tilde{V}_k = k^{-d}V_k$ is the dimensionless scaling potential, k is the running momentum, $\alpha_d = \Omega_d/(2(2\pi)^d)$, and $\Omega_d = 2\pi^{d/2}/\Gamma(d/2)$ is the d-dimensional solid angle. The tilde denotes dimensionless quantities which are obtained from the dimensionful ones via multiplication by an appropriate power of k, to take away their dimension. The dimensionful and dimensionless quantities are related by the relations

$$\tilde{\beta} = k^{(d-2)/2} \beta$$
, $\tilde{m} = m/k$, $\tilde{u} = k^{-d} u$. $\tilde{\phi} = k^{-(d-2)/2} \phi$. (3.2)

It is important to note that the proposed RG treatment gives the same flow equations for each form of the MSG model, i.e., for our main model given in eq. (2.4), as well as the variants discussed in eqs. (B.2) and (B.3), because field independent terms do not change the running, and the RG equation is symmetric under the $u \to -u$ transformation.

The two-dimensional MSG model has already been considered using a momentum shell RG scheme in refs. [77–80]. Here, we extend these studies to d=4 dimensions. We look for the solution of eq. (3.1) in the functional form of the MSG model.

We pause here to point out that the function $V_k(\phi)$, in zeroth order in ϕ , is a function only of k; we denote it as $V_k(0)$. Some comments and speculations on the RG evolution of the field-independent, constant term $V_k(0)$ are presented in appendix D. From one side, the precise form of the function $V_k(0)$ is irrelevant for our following discussion, in the sense that none of our results of the main text depend on it. From the other side, we alert the reader that if one aims at a determination of the free energy in a flat background or of the cosmological constant in a general non-flat background, then the problem of unambiguously determining $V_k(0)$ has to be seriously considered. A few remarks on this point, beyond the discussion in appendix D, are in order. Namely, it is known that in principle, the nonperturbative RG method for the MSG (see refs. [64, 65] and appendix C), cannot be used in order to determine the RG evolution of the field-independent, k-dependent term $V_k(0)$, uniquely. Upon integration, such terms amount to field-independent contributions to the total action integral. The reason for the emergence of the field-independent, k-dependent terms lies in the fact that properties are imposed on the regulator [see eq. (C.4) and eqs. (13)—(15) of ref. [81]]. This implies that the solution of the RG equation for the potential $V_k(\phi)$ recovers the bare action in the UV only up to a k-dependent, but field-independent term. The problem reflects the fact that the field-independent, but renormalization-scale dependent terms can lead to an (unphysical) divergence of $V_k(0)$ in the UV limit, as explained in section 2.3 of ref. [81]. This unphysical behavior necessitates the introduction of subtraction terms if any meaningful information is to be obtained. In appendix D, we discuss possible subtractions. We finally observe that the result one may obtain for $V_k(0)$ in the effective action would be proportional to the free-energy density of the inflaton field in the flat background limit. A systematic investigation of the conditions that could unambiguously fix the subtraction scheme in the general case with curved space-time is currently lacking, to the best of our knowledge, and it would be extremely desirable. For the purposes of the present paper, our view is to choose a renormalization scheme by which we obtain observationally acceptable results for the RG running of the potential. Provided we have at least one false vacuum in the UV, we conjecture that these results, in the IR, even become independent of the details of the particular field-theoretical model once that, due to the RG running, the potential starts to flatten and becomes convex. The question of whether the chosen RG scheme is also capable of describing the RG running of the field-independent term is of lesser importance in the mentioned context.

Let us consider, then, the field-dependent terms, for which the RG equation used by us requires no subtractions or modifications. So, substituting expressions given in eqs. (2.4), (B.2) and (B.3) into eq. (3.1), one can match the periodic and non-periodic terms. The right-hand side is periodic, and therefore, the non-periodic terms are

$$\tilde{m}^2 \tilde{\phi}^2 + k \partial_k \left(\frac{1}{2} \tilde{m}^2 \tilde{\phi}^2 \right) - \tilde{u} \tilde{\phi} \sin(\tilde{\beta} \tilde{\phi}) \frac{d-2}{2} \tilde{\beta} + \tilde{u} \tilde{\phi} \sin(\tilde{\beta} \tilde{\phi}) \left(k \partial_k \tilde{\beta} \right) = 0.$$
 (3.3)

These also split into two separate equations, one for the $\tilde{\beta}$ and another for \tilde{m} , as one can show by investigating the purely polynomial and trigonometric terms separately. Thus, from the non-periodic part, one immediately gets the flow equations for $\tilde{\beta}$ and for \tilde{m} ,

$$k\partial_k \tilde{\beta}_k = \frac{d-2}{2}\tilde{\beta}_k \qquad \rightarrow \qquad \tilde{\beta}_k = \beta k^{\frac{d-2}{2}},$$
 (3.4a)

$$k\partial_k \tilde{m}_k^2 = -2\tilde{m}_k^2 \qquad \to \qquad \tilde{m}_k^2 = m^2 k^{-2}. \tag{3.4b}$$

These solutions imply that according to the lowest-order RG study of the MSG potential, the corresponding dimensionful quantities (m,β) remain unchanged during the RG flow. Therefore, only the dimensionful Fourier amplitude u changes when the cutoff scale k is decreased from its (high-energy) pre-inflationary value Λ towards the (low-energy) inflationary stage, describing the transition toward a convex potential.

The flow equation for u can be obtained from the remaining periodic terms,

$$-\cos(\tilde{\beta}\tilde{\phi})(d+k\partial_k)\tilde{u} = \frac{2\alpha_d}{d} \frac{1}{(1+\tilde{m}^2+\tilde{u}\tilde{\beta}^2\cos(\tilde{\beta}\tilde{\phi}))}.$$
 (3.5)

Although the right-hand side of (3.5) contains higher Fourier modes, here we focus on the single-mode approximation, which means that after the Fourier expansion of both sides of (3.5), only the single cosine terms are kept and compared. The result of this procedure is the flow equation for the Fourier amplitude \tilde{u} which reads as

$$(d+k\partial_k)\tilde{u}_k = -\frac{4\alpha_d}{d} \frac{1}{\tilde{\beta}_k^2 \tilde{u}_k} \left(1 - \sqrt{\frac{\left(1 + \tilde{m}_k^2\right)^2}{\left(1 + \tilde{m}_k^2\right)^2 - \tilde{\beta}_k^4 \tilde{u}_k^2}} \right). \tag{3.6}$$

Solving these partial differential equations for the couplings simultaneously, one determines how the potential of the MSG model depends on the running scale.

It is useful to rewrite eq. (3.6) in terms of dimensionful quantities, with the result

$$k\partial_k u_k = -\frac{4\alpha_d}{d} \frac{k^{d+2}}{\beta^2 u_k} \left(1 - \sqrt{\frac{(k^2 + m^2)^2}{(k^2 + m^2)^2 - \beta^4 u_k^2}} \right). \tag{3.7}$$

While u_k is running, the two other dimensionful parameters (β, m) are constant over the flow, according to eq. (3.4). Let us linearize eq. (3.7) around the Gaussian fixed point assuming that $\beta^2 u_k/(k^2 + m^2) \ll 1$, with the result

$$k\partial_k u_k = -\frac{4\alpha_d}{d} \frac{k^{d+2}}{\beta^2 u_k} \left(1 - \sqrt{\frac{1}{1 - \beta^4 u_k^2 / (k^2 + m^2)^2}} \right) \approx \frac{2\alpha_d}{d} \frac{k^{d+2}}{\beta^2 u_k} \frac{\beta^4 u_k^2}{(k^2 + m^2)^2}, \quad (3.8)$$

which can be further simplified if the (dimensionful) mass is much smaller than the running RG scale, i.e., $m^2 \ll k^2$, in which case the flow equation reads as

$$k\partial_k u_k \approx \frac{2\alpha_d}{d} k^{d-2} \beta^2 u_k \,. \tag{3.9}$$

The latter is the linearized RG flow equation for the massless sine-Gordon model. Its solution can be obtained analytically and for d=4 dimensions it has the following form ($\alpha_{d=4}=1/16\pi^2$)

$$u_k = u_\Lambda \exp\left[\frac{\beta^2}{64\pi^2}(k^2 - \Lambda^2)\right]$$
 (3.10)

where u_{Λ} is the initial value for the Fourier amplitude at the UV scale Λ . Within the context of our investigations, an obvious choice is the Planck scale, $\Lambda = \Lambda_p = 2.4 \times 10^{18} \,\text{GeV}$. However, we should emphasize that our strategy here is a little different from what is usually employed in an RG analysis. Namely, while the UV scale of our analysis is the Planck scale, this is not the scale where we match the parameters of our model against astrophysical

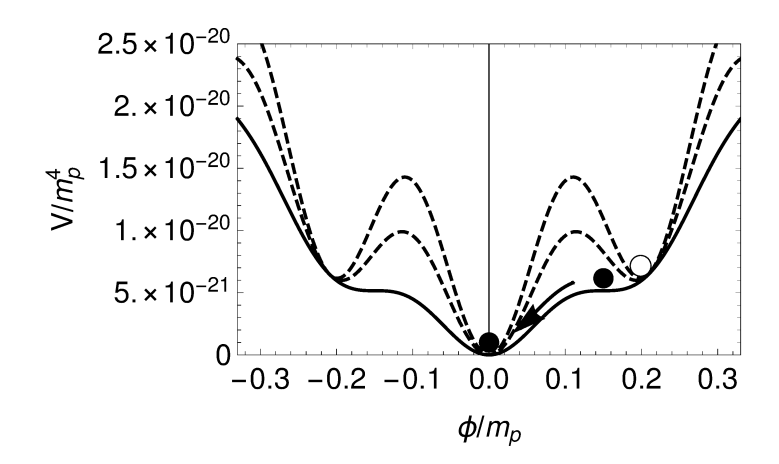


Figure 2. Potential of the MSG model (2.4) at various RG scales. The solid line stands for the potential at the scale of inflation ($k_i = 2.0 \times 10^{13} \,\text{GeV}$). The values of the potential parameters have been calculated by the acceptance region in figure 4 with the choice $\hat{\beta} = 30$. Using eq. (3.19) the normalized parameters are $\hat{m} = 5.4 \times 10^{-10}$, $\hat{u} = 1.5 \times 10^{-21}$, $\hat{\beta} = 30$ which yield the solid line that represents the potential over the whole inflationary period, where the VeV (full black circle) rolls down inducing inflation. The dashed lines correspond to UV values (pre-inflation), obtained by RG considerations using eq. (3.10), see the discussion in section 3.1.

observations. Instead, we fix the value of the running Fourier amplitude u_k and also the value of the constant dimensionful frequency β and mass m at the scale of inflation k_i , e.g., at the GUT scale, $k_i \sim k_{\rm GUT} = 2 \times 10^{16} \,\text{GeV}$, where one can match them with the slow-roll parameters (u_0, β_0, m_0) . Once more, we emphasize that it is the scale of inflation k_i , i.e., the starting point of the slow-roll, not the Planck scale, where the parameters are matched, according to

$$u_{k_i} = u_0, \quad \beta = \beta_0, \quad m = m_0.$$
 (3.11)

Once these values are fixed, one can easily obtain the initial condition u_{Λ} by using for example the solution (3.10) (in its region of applicability, as discussed above) or in more general the solutions [eq. (3.4)] of the RG flow equations. As a final result, the RG scaling of the dimensionful Fourier amplitude u_k is fully determined.

3.2 Pre-inflationary period and RG running

Let us now study the effects of quantum fluctuations in the pre-inflationary period by applying the RG method for the MSG model in d=4 dimensions. The quadratic LFI potential has no RG evolution at all, i.e., the dimensionful mass remains unchanged, so that the dimensionless mass has a trivial RG scaling. Instead, as discussed, the MSG model has a non-trivial RG scaling because of the periodic term which evolves under RG transformation; yet, the dimensionful mass term again has no RG evolution, as implied by eq. (3.1). Let us now use the results of the RG analysis in order to discuss a possible mechanism for inflation. For the sake of simplicity, we consider MSG potentials with parameters fixed by the slow-roll study. Suppose that at very high energy scales (deep UV region) in the pre-inflationary period, the VeV is situated in the second minimum of the MSG potential [see figure 2 for the model given in eq. (2.4) and appendix B for the other two variants, given in eqs. (B.2) and (B.3)].

RG evolution forces the potential to tend a convex one valid for any potential, as shown in appendix C, and so the MSG potential becomes shallow at the scale of inflation. At

this stage, the VeV starts to roll down towards the real minimum, inducing inflation. We find that the inclusion of quantum fluctuations leads to a strong renormalization of the inflationary potential, eventually leading to the disappearance of the false vacua trapping the VeV expectation in the pre-inflationary period, thereby inducing inflation.

3.3 Inflationary period and slow roll

Let us now discuss the picture emerging for the inflationary period using the MSG model. In order to follow the conventions of inflationary cosmology in the slow-roll study we use reduced Planck units

$$c \equiv \hbar \equiv 1, \qquad m_p^2 = \frac{1}{8\pi G} \equiv 1.$$
 (3.12)

Thus, dimensionless quantities of the MSG model in the framework of the slow-roll analysis are understood as

$$\hat{u} = \frac{u_0}{m_p^4}, \qquad \hat{\beta} = \beta_0 \, m_p, \qquad \hat{m} = \frac{m_0}{m_p}, \qquad \hat{\phi} = \frac{\phi}{m_p},$$
 (3.13)

where u_0 , β_0 and m_0 are the dimensionful couplings fixed at the scale of inflation k_i , i.e., at a scale commensurate with or even below the GUT scale, and not at the Planck scale. In passing, we note that $m_p = 2.4 \times 10^{18} \,\text{GeV}$, while the GUT scale is at $k_{\text{GUT}} = 2 \times 10^{16} \,\text{GeV}$, so that

$$\frac{k_{\text{GUT}}}{m_p} \approx \frac{1}{120} \,. \tag{3.14}$$

Of course, in Planck units, the dimensionful and dimensionless parameters (which are commonly referred to as the "reduced" quantities in metrology) assume the same numerical values. The slow-roll analysis fixes the (dimensionless) parameters, and so we can easily restore the dimension later. In Planck units, the slow-roll conditions are the following

$$\epsilon \equiv V'^2/(2V^2) \ll 1 \,, \qquad \eta \equiv V''/V \ll 1 \,, \tag{3.15a} \label{epsilon}$$

which have to be fulfilled by a suitable potential for a prolonged exponential inflation with slow roll down. The e-fold number

$$N \equiv -\int_{\phi_i}^{\phi_f} d\phi \frac{V}{V'} \tag{3.16}$$

should be in the range

$$50 < N < 60. (3.17)$$

Here, ϕ_i and ϕ_f are the initial and final configurations of the field, respectively.

The power spectra of scalar $(\mathcal{P}_{\mathcal{S}})$ and tensor $(\mathcal{P}_{\mathcal{T}})$ fluctuations can be characterized by their scale dependence, i.e., $\mathcal{P}_{\mathcal{S}} \sim k^{n_s-1}$, where k is the comoving wave number. Then, slow-roll parameters are encoded in expressions for the scalar tilt $n_s - 1 \approx 2\eta - 6\epsilon$ and for the tensor-to-scalar ratio $r = \mathcal{P}_{\mathcal{T}}/\mathcal{P}_{\mathcal{S}} \approx 16\epsilon$, which can be directly compared to CMBR data [6].

We here initially focus on the first variant of the MSG model, given in eq. (2.4). The explicit form of the potential during the inflationary period is reported as a solid line in figure 2 (see also figure 7 and figure 8 and appendix B for the other two variants of the MSG model). Let us first compare results obtained from natural inflation, i.e., sine-Gordon and MSG models, for various values of the frequency. As shown in figure 3, the MSG model provides more reliable results. Moreover, the ratio \hat{u}/\hat{m}^2 and the frequency $\hat{\beta}$ can be fixed

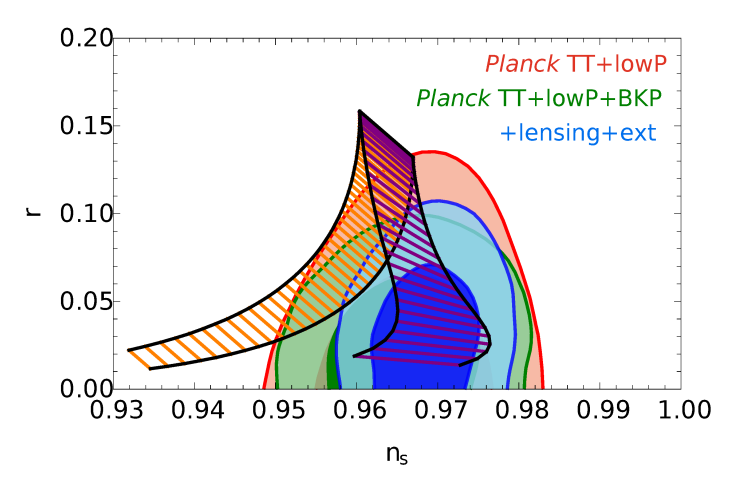


Figure 3. Scalar tilt n_s and tensor-to-scalar ratio r derived for various frequencies (i) for the natural inflation model (orange line segments to the left) and (ii) for the MSG model given in eq. (2.4) with fixed ratio $\hat{u}/\hat{m}^2 = 1/(0.22)^2$ (purple line segments in the middle). As evident from the uppermost orange line segment, the two models give identical results for $\hat{\beta} = 0$. Different purple line segments result from different values of $\hat{\beta}$ (for the massive model). Both are compared to results of the Planck mission [11–13] where dark color regions stand for 95% CL and the light color regions correspond to 68% CL. The notation BKP stands for the combined data from BICEP2/Keck Array and Planck Collaborations. We adopt the following labels for likelihoods: (i) Planck TT denotes the combination of the TT likelihood at multipoles $l \leq 30$; (ii) Planck TT+lowP further includes the Planck polarization data in the low-l likelihood and "ext" is used for external data, e.g. baryon acoustic oscillations (BAO). As evident from eq. (3.21), the best acceptance region for Planck data is reached for a value of $\hat{\beta} \approx 0.3$ (for fixed ratio $\hat{u}/\hat{m}^2 = 1/(0.22)^2$) with the massive model. More data (various color schemes) evidently put more stringent constraints on the acceptance region for n_s and r. The "rungs" of the latter correspond to the range (3.17) indicated for the e-fold number N.

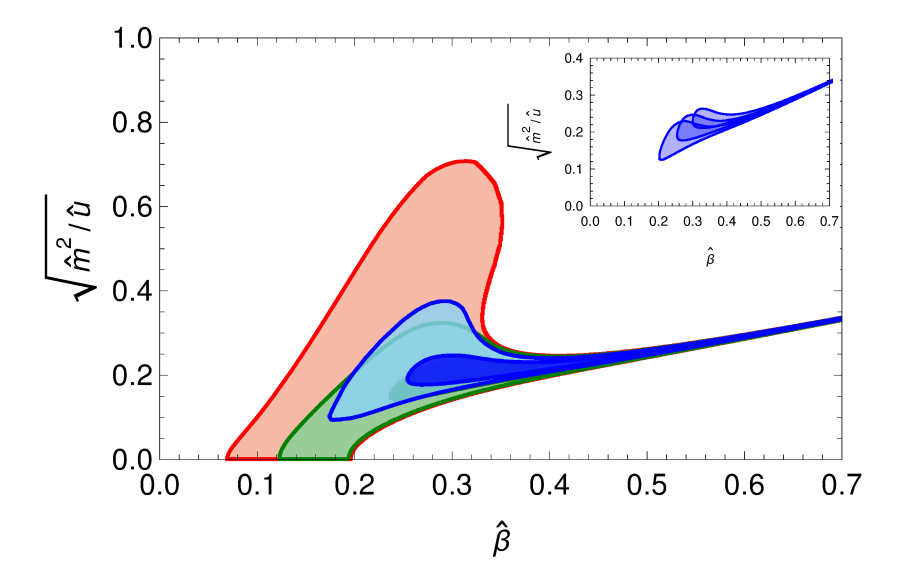


Figure 4. Regions of the parameter space of the MSG model given in eq. (2.4) are indicated by different colors corresponding to a different level of acceptance for folding number N=55. The dark blue region gives the best fit to Planck data. The inset shows the best acceptance regions for N=50,55,60.

by choosing the best fit to observations (see figure 3). In figure 4, we indicate regions of the parameter space of the MSG model with different colors corresponding to different levels of acceptance.

For the plot in figure 2 and elsewhere, it is necessary to fix the scale of the ordinate axis for the potential. This is done as follows. Let ϕ_i denote the VeV of the value of the field ϕ at the onset of the slow-roll, i.e., the VeV of the potential at the very point in the RG analysis where the "false" vacuum disappears and the slow-roll begins. Writing eq. (2.4) as

$$V_{\text{MSG}}(\phi) = u \left(\frac{1}{2} \frac{m^2}{u} \phi^2 + [1 - \cos(\beta \phi)] \right),$$
 (3.18)

and in consideration of eq. (3.21) below, one immediately sees that fixing the absolute value of the potential at $\phi = \phi_i$ is tantamount to choosing a particular absolute normalization for the value of $u = u_{k_i}$. Depending on the value obtained for the tensor-to-scalar ratio r in the acceptance region [see also figure 3], the scale of inflation can be commensurate with the GUT scale, i.e., $k_i \sim k_{\text{GUT}} = 2 \times 10^{16} \text{GeV}$. Here, we fix the absolute normalization factor for the potential so that the exact condition [see eq. (23) of ref. [83] and eq. (218) of ref. [58]],

$$V(\phi_i) \equiv \frac{r}{0.01} (10^{16} \,\text{GeV})^4,$$
 (3.19)

is being met. The tensor-to-scalar ratio r is given by the slow-roll parameters, and determined by the $\hat{\beta}$ -dependent acceptance region; the scale of inflation [which is determined by the tensor-to-scalar ratio for a single field inflation, see the text above eq. (218) of ref. [58]] is defined as

$$V(\phi_i) \equiv k_i^4, \qquad k_i = \left(\frac{r}{0.01}\right)^{\frac{1}{4}} 10^{16} \text{ GeV}.$$
 (3.20)

Let us note, by way of example, that according to figure 3, the slow-roll study of the MSG model with the fixed ratio $\hat{u}/\hat{m}^2 = 1/(0.22)^2$ gives the fit parameters $\hat{\beta} \approx 0.3$ and $r \approx 0.05$ for the acceptance region, and so, in this case, the scale of inflation, $k_i = 1.5 \times 10^{16}$ GeV, is around the GUT scale.

The theoretical predictions obtained from the MSG model are in an excellent agreement with observations. Surprisingly, we can use the results of the slow-roll study in order to fix the parameters of the MSG model at the scale of inflation. There are two regions in the parameter space of the MSG-type models where one finds good agreement with observations, and we will discuss these two regions separately.

3.4 Fit to experimental data for small β

The ratio and frequency taken from the dark blue region give the best fit to Planck data and the third parameter (the mass) can be fixed by the power spectrum normalization, i.e., by eq. (3.19). Let us use this scenario to fix the admissible parameter regions of MSG-type models for small β . The best dimensionful values for the MSG model (2.4) taken from the slow-roll study read can be read off from figures 3 and 4. In particular, the blue "blob" region in figure 4 can be identified as the start point of a nearly straight line in parameter space, along which the following condition holds,

$$\frac{\hat{u}\hat{\beta}^2}{\hat{m}^2} = \frac{u_0\beta_0^2}{m_0^2} \approx \frac{0.3^2}{0.22^2} > 1. \tag{3.21}$$

Furthermore, the blue "blob" is easily located around the value $\hat{\beta} \approx 0.3$ in figure 4, which, together with the normalization condition (3.19), leads to the following numerical values for the fit parameters,

$$\hat{m}^{\text{small}} \approx 5.92 \times 10^{-6}$$
 \Rightarrow $m_0^{\text{small}} \approx 1.42 \times 10^{13} \,\text{GeV}$, (3.22a)
 $\hat{u}^{\text{small}} \approx 7.24 \times 10^{-10}$ \Rightarrow $u_0^{\text{small}} \approx 2.4 \times 10^{64} \,\text{GeV}^4$, (3.22b)
 $\hat{\beta}^{\text{small}} \approx 0.3$ \Rightarrow $\beta^{\text{small}} \approx 1.25 \times 10^{-19} \,\text{CeV}^{-1}$ (3.22c)

$$\hat{u}^{\text{small}} \approx 7.24 \times 10^{-10} \qquad \Rightarrow \qquad u_0^{\text{small}} \approx 2.4 \times 10^{64} \,\text{GeV}^4 \,, \tag{3.22b}$$

$$\hat{\beta}^{\text{small}} \approx 0.3$$
 $\Rightarrow \beta_0^{\text{small}} \approx 1.25 \times 10^{-19} \,\text{GeV}^{-1}$. (3.22c)

For the particular choice of the fit parameters exemplified in figure 3, the scale of inflation is found to be of the same order-of-magnitude as the GUT scale, with the result $k_i = 1.5 \times 10^{16} \, \text{GeV}$, as already indicated above. Further details of the acceptance regions can immediately be read off from figures 3 and 4. One can conclude that the slow-roll study for small β provides parameters for the MSG model where the relation $\frac{u_0\beta_0^2}{m_0^2} > 1$ always holds [independent of the variant of the MSG model considered; see eqs. (2.4), (B.2), and (B.3)].

Finally, let us note that the dimensionful parameters of the MSG model determined by the slow-roll analysis in the small β region are small compared to the GUT scale, see eq. (3.22a), and thus, the approximate solution (3.10) of the RG flow equation (3.7) can be used to obtain the RG scaling of the potential and to extrapolate towards higher energy scales.

It is easy to check that, during the RG flow, down from the Planck to the GUT scale, the expression $\beta k = \beta_0 k$ assumes values in the range

$$\hat{\beta} \frac{k_{\text{GUT}}}{m_p} < (\beta_0 \, k) < \hat{\beta} \,. \tag{3.23}$$

The change in the potential during the RG, i.e., during the scaling from the Planck to the GUT scale, has to be substantial in order for our proposal to be physically meaningful. From eqs. (3.10) and (3.14), we infer that

$$\chi = \frac{u_{m_p}}{u_{k_{GUT}}} = \exp\left[\frac{1}{64\pi^2} \left(\hat{\beta}^2 - \frac{\hat{\beta}^2}{120^2}\right)\right]. \tag{3.24}$$

In the region

$$\hat{\beta} \gtrsim 30, \qquad \chi \gtrsim 4.2,$$
 (3.25)

the ratio χ implies a (more than) four-fold change in the amplitude u. This constitutes the (more favorable) region of large $\hat{\beta}$ which we study in the following. The only other way to reconsider the region of small $\hat{\beta}$ is to postulate an RG running over super-Planckian scales, which however, seems somewhat problematic even for the cosmological era under consideration here.

3.5 Fit to experimental data for large β

In order to investigate the (favored) region of large $\hat{\beta}$, we have carried out numerical calculations for all versions of the MSG model. Those three versions [given in eqs. (B.2), (B.3) and (B.10), where the periodic term has the same sign, have absolutely equivalent behavior in the range $\hat{\beta} \gtrsim 1.0$, i.e., their best acceptance regions overlap (see figure 5).

The first version (2.4) produces the same qualitative result, but with a slightly different slope. So, one can conclude that in the large frequency range, relevant for fixing the parameters of the model at the very beginning of inflation, all versions of the MSG model produce the same initial value for the VeV.

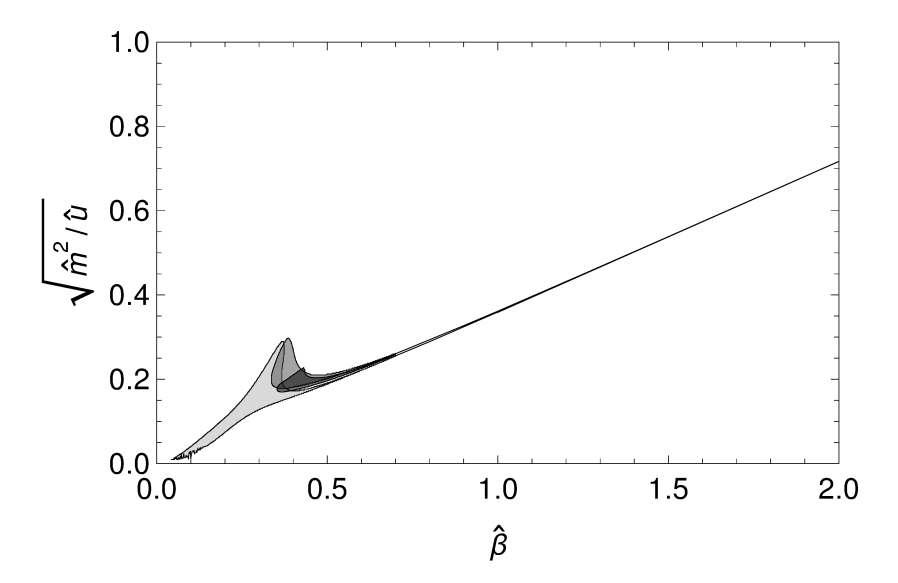


Figure 5. The best acceptance regions for three variants of the MSG model (B.2), (B.3) and (B.10) coincide in the limit of large $\hat{\beta}$.

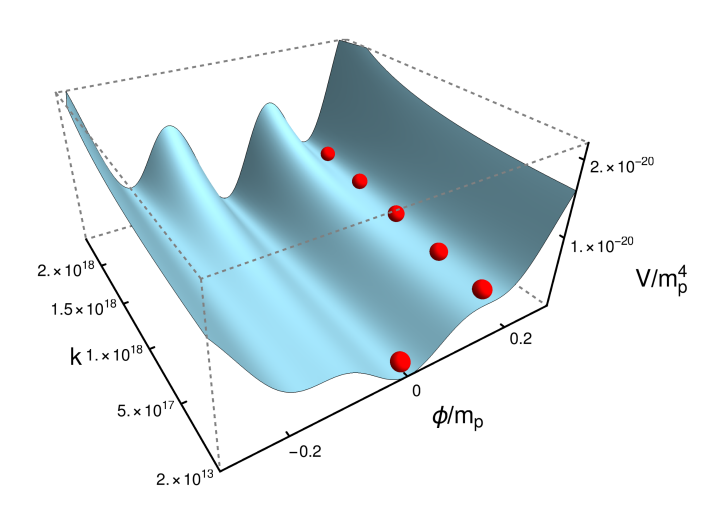


Figure 6. The RG scaling of the MSG potential is shown from the Planck scale towards the scale of inflation for $\hat{\beta} = 30$. The MSG potential at $k_i = 2.0 \times 10^{13} \,\text{GeV}$ is fixed by the slow-roll analysis. The red ball denotes the VeV which is trapped in a false vacuum at the Planck scale and due to RG running it is released at the scale of inflation to roll down to the real ground state.

We note that the scale of inflation k_i depends on the particular choice of $\hat{\beta}$. For small values of $\hat{\beta}$, the inflation occurs at the GUT scale. For large values, i.e., for $\hat{\beta} \gtrsim 1.0$ the scale of inflation is smaller than the GUT scale. For $\hat{\beta} \gtrsim 30$, one finds $k_i = 2.0 \times 10^{13} \,\text{GeV}$. In this particular case, the RG running leads to a pronounced sufficient decrease in the Fourier amplitude $u(k=m_p)/u(k_i) \gtrsim 4.2$. A visual representation of the change is given in figure 6, where the change in the shape of the potential against the running RG scale k is plotted for $\hat{\beta} = 30$ [the corresponding 2D figure is figure 2].

Finally, let us add a few remarks on the preferred values of $\hat{\beta}$ that result from our analysis. On the one hand, if one takes the view that the vacuum should be "safely" trapped in the false vacuum at the Planck scale, then the change in the effective potential from the

Planck scale down to the scale of inflation has to be substantial. Under these assumptions, a minimum choice would be $\hat{\beta} \gtrsim 30$, since otherwise there is no sufficiently large change in the shape of the potential caused by the RG running between the Planck scale and the scale of inflation; hence the RG running cannot induce inflation. On the other hand, if $\hat{\beta} \sim 300$, then the scale of inflation exceeds the GUT scale by more than four orders of magnitude, which is certainly counter-intuitive.

This observation is important because the parameters of the model are fixed by comparison to experiment [11–13], with the exception of $\hat{\beta}$. Once $\hat{\beta}$ is chosen and the normalization condition (3.19) is implemented, all other parameters of the model are fixed.

4 Conclusions

We have demonstrated, by the RG study of the MSG model, that the RG running of the parameters in the pre-inflation period naturally provides us with a flattening of the potential, i.e., it tends to a convex shape which allows the field to roll down to the true vacuum classically (see figure 2). We argue that the MSG model is a viable cosmological model, and, if confronted with the very recent Planck data, gives very good agreement. Our results also show that it does not matter if we add a constant term to the MSG model, as evident from the results obtained using variants of the MSG model. Furthermore, we argue that the proposed RG-induced mechanism should work for any inflationary potential with concave regions. We merely choose the three variants of the MSG model, and the V_{ϕ^6} theory to illustrate the generality of our arguments. Thus, the very general statement holds that due to convexity, the false vacuum should disappear at a certain lower energy scale, and the VeV which is trapped in the false vacuum at high energies, should start to roll down towards the real ground state when the false vacuum disappears.

However, it is important to note that in a realistic demonstration of the change from concavity to convexity of the inflationary potential in the RG context, one should consider some particular GUT with a given matter content. This is particularly significant in the pre-inflationary epoch. We do not pursue such a study here, however, we here note that other fields do not change the RG running of the inflation potential drastically, so that the effective (scalar) potential in the IR should be convex.

Let us put our findings into a wider context. Small-field inflationary models are not in favor since initial conditions are more problematic for small-field inflation. Hybrid inflationary models are not supported or almost totally excluded by recent Planck data since they require $n_s > 1$ (see refs. [83, 84]), but we know from Planck data that $n_s < 1$. Therefore, large-field models seem to be better candidates but in general, they have a weakness, namely, their large initial value for the VeV which makes it difficult to support them by a particle-physics model. The importance of our method proposed here is that so-called "chaotic", large-field inflationary models could be supported by a particle-physics origin since there is no need for large field fluctuations at the scale of inflation. RG running induces inflation from a false vacuum where the VeV is trapped at very high energies (much higher than the scale of inflation); in this region, it is permissible to assume large field fluctuations.

The method of RG-running induced inflation, as we show, determines a unique initial value as a starting point for the VeV, and so, it explains why the inflaton field starts in the particular slow roll domain. By a unique initial value as a starting point for the VeV, we mean that in the RG-induced inflationary scenario, the VeV, i.e., the false vacuum which is the initial value for the slow-roll depends only on the shape of the potential. Other

scenarios often depend on the random process of quantum fluctuations to excite the field to the initial value of the slow-roll. However, apart from the quantum fluctuations, the RG induced inflation has a unique initial value and solves this problem. In other words, no large amplitude fluctuations are needed at the energy scale of inflation (the VeV is assumed to be trapped in a false vacuum at very high energies). This fact may help to build up inflation with the same rate at various regions of space and solve the initial-value problem.

Acknowledgments

This work was supported by ÚNKP-17-3 New National Excellence Program of the Ministry of Human Capacities, the National Science Foundation (Grant PHY-1710856) and the Deutsche Forschungsgemeinschaft (DFG, German Research Foundation) via Collaborative Research Centre "SFB1225" (ISOQUANT) and under Germany's Excellence Strategy "EXC-2181/1-390900948" (the Heidelberg STRUCTURES Excellence Cluster). Useful discussions with Z. Trocsanyi and G. Somogyi are gratefully acknowledged. N. D. is grateful to F. Bianchini and J. Rubio for useful discussion in the early stages of this work. The CNR/MTA Italy-Hungary 2019-2021 Joint Project "Strongly interacting systems in confined geometries" also is gratefully acknowledged.

A RG running and Hubble time

A few illustrative remarks on RG evolution and time dependence are in order. Here, we by no means assume that the RG, eo ipso, induces a time-dependence. However, it is still permissible to associate the running momentum scale with the cosmological time. The essential idea to argue in favor of this hypothesis has been formulated in refs. [18–27]: if one considers the Universe at age t, then it is forbidden to assume fluctuations with a frequency higher than 1/t. So, the mode integration, which is the cornerstone of the functional RG method, has to be stopped at a scale $k \approx 1/t$. For further details, one may consult refs. [18–27]. Indeed, a number of recent papers [35–49] use this idea.

Let us put this statement into context. We first recall that the original idea to relate the RG to a blocking construction in real space (which amounts to the integration of higher momentum shells in momentum space) has been formulated by Kadanoff [see eqs. (1)–(11) of ref. [55]] and Wilson [see eq. (17) of ref. [56]]. The notion was that only some specific details of the microscopic theory should be important for the prediction of the same critical behavior at large distance scales (within a given "universality class"). In order to describe the connection to time evolution in the Early Universe, one imagines, e.g., a tiny crystal of a substance forming, and then, growing fast. At first, the interactions within the crystal are described by the microscopic interaction, but then, as the crystal grows fast, the correlation functions are those of the effective, low-energy theory. In the same right, we can assume the Universe to grow over time, thus realizing the Wilson blocking construction in real space, as the universe expands. That is the idea behind the concepts formulated in refs. [18–27]. For an excellent review on the blocking construction in momentum space and the functional RG, we refer to ref. [57].

Indeed, invoking the concepts of homogeneity and isotropy, it was argued in refs. [18–27] that k can only depend on the cosmological time, and that the correct identification is given by a functional relationship $k(t) = \xi/t$, where ξ is a positive constant of order unity. It would thus be assumed that the RG scale k is a related to the inverse of the age of the Universe

which is identified by the Hubble time $t \sim H^{-1}$ where H(t) is the time-dependent Hubble parameter. However, we should stress that the precise details of the identification are not important for the fitting of the parameters of our field-theoretical model to astrophysical observations, which will be described in the following. All we require is that the momentum scale k be a monotonically decreasing function of a more general time scale, say, τ , the latter of which constitutes some kind of cosmological time parameter, e.g., a comoving (particle) horizon. An alternative natural identification would thus be based on the conformal time $d\tau = dt/a(t)$, where a(t) is the scale factor of the FLRW metric. One finds the following expression for the comoving (particle) horizon,

$$\tau = \int_0^t \frac{dt'}{a(t')} = \int_0^a d\ln a \, \frac{1}{aH}$$
 (A.1)

[see eq. (36) of ref. [58]]. Here, a(t) is the scale factor of the FLRW metric. The time-dependence of the comoving Hubble radius is known from the solution of the FLRW equation, $(aH)^{-1} = H_0^{-1}a^{1+3w}$. For the radiation (i.e., relativistic matter) dominated case, w=1/3 and $a(t) \sim t^{1/2}$, while for the non-relativistic matter dominated epoch, we have w=0 and $a(t) \sim t^{2/3}$. For the dark-energy dominated regime, one has w=-1 and $a(t) \sim \exp(Ht)$. The comoving Hubble radius is found to be an increasing parameter of time except for the dark-energy dominated regime (see table 2 of ref. [58]). For our investigations, it is important that $\tau \sim a^{1+3w}$ is monotonically increasing with time in the radiation-dominated regime ($\tau \sim a \sim t^{1/2}$) and also in the matter-dominated case ($\tau \sim a^{1/2} \sim t^{1/3}$). In our RG-supported picture, the precise functional relationship between the momentum scale k of the RG and the cosmological time parameter τ is of lesser importance in the the pre-dark-matter period. The same qualitative and, for our investigations, quantitative picture results if one universally assumes that the RG scale k is a monotonically decreasing function of the age of the very early Universe. Favorable and intriguing observations for suitable parameter regions are reported in sections 3.5.

B Slow-roll studies of alternative models

B.1 Slow-roll study of the MSG model

In the framework of the MSG model, we consider the following variants of the model originally proposed in eq. (2.4),

$$V_{\text{MSG}_1}(\phi) = \frac{1}{2}m^2\phi^2 + u\left[1 - \cos(\beta\phi)\right],\tag{B.1}$$

$$V_{\text{MSG}_2}(\phi) = \frac{1}{2}m^2\phi^2 + u\left[\cos(\beta\phi) - 1\right],$$
(B.2)

$$V_{\text{MSG}_3}(\phi) = \frac{1}{2}m^2\phi^2 + u\left[\cos(\beta\phi) - 1\right] - V_0,$$
(B.3)

where the second version differs from the first only by the sign of the u. The third version has an additional constant V_0 to keep the minima of the potential at zero (which can be achieved by a possibly k-dependent, but field-independent subtraction term V_0).

In principle, one might argue that the slow-roll analysis of (B.1), with a negative value for the coupling u, should give the same result as the slow-roll analysis of (B.2) with the same magnitude, but opposite sign, of the coupling u, and vice versa. This conjecture could

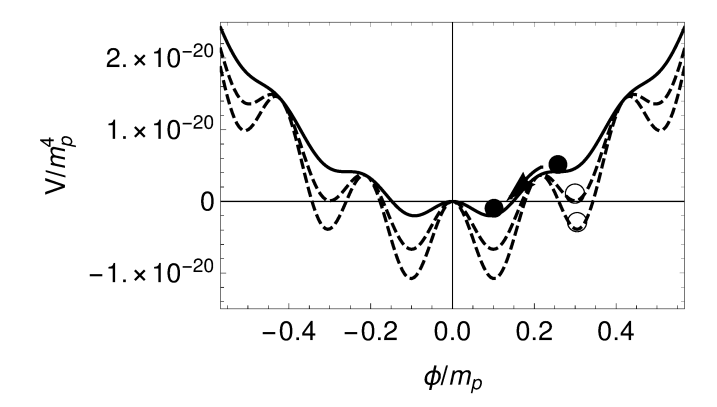


Figure 7. The same as figure 2, but for the second version of the MSG model (B.2). Here the normalized parameters, corresponding to the solid line, are $\hat{m} = 4.0 \times 10^{-10}$, $\hat{u} = 1.4 \times 10^{-21}$, $\hat{\beta} = 30$ which have been derived from the acceptance region of figure 5 using the slow-roll study with $\hat{\beta} = 30$.

be based on the fact that models (B.1) and (B.2) turn into each other upon the replacement $u \to -u$. However, during our numerical analysis, we keep u positive. Hence, there is a difference between the variants, since the slow-roll analysis is not symmetric under the sign change of u. In particular, both $\epsilon = 1/2(V'/V)^2$ and $\eta = V''/V$ depend on the sign of u. An essential difference between the MSG variants (B.1) and (B.2) is the position of the global minima. For the model (B.1), the potential has a global minimum at zero, while for (B.2), it has two degenerate global minima, and a local maximum at zero. Therefore, the position of the expectation value of the field (ϕ_f) after the inflation, and other results of the slow-roll analysis, are also different for the two variants.

An essential observation is that we can, colloquially speaking, identify u = u(k) with an "oscillation amplitude" of the field as it multiplies the cosine term. In some sense, one can thus argue that the slow-roll study of the variants of the MSG model depends more on the magnitude of u than on its sign in the large β limit. That is because, if one chooses u or -u, and a given value of m and β , one gets a potential whose first "false" vacuum lies approximately at the same position in the UV for large β values. The "swing factor" of the potential does not depend on the sign of u, only on the magnitude (modulus) of u. Therefore, similar slow-roll results are expected for the variants of the MSG model in the large β limit which is demonstrated in figure 5.

However, when one evolves the potential into the IR, the difference become apparent: the minimum of (B.1) migrates to $\phi = 0$, while the minimum of the model (B.2) goes to a nonvanishing vacuum expectation value $\phi = \phi_0$. We refer to figures 6, 11 and 12 for three-dimensional graphics respresenting the RG evolution of the potentials, verifying the above, intuitive arguments.

In more general terms, it is interesting to observe that the variants (B.1) and (B.3) are expected to give identical slow-roll results in the limit of vanishing mass, i.e., $m \to 0$; compare figure 4 and figure 10 in the limit of vanishing mass. This becomes evident after taking the limit $m \to 0$ in (B.3) while the constant term, for $m \to 0$, is fixed as $V_0 = -2u$. The variants (B.1) and (B.3) then become identical when the field variable is shifted according to $\phi \to \phi + \pi/\beta$.

Before we come to the slow-roll analysis, we briefly remark that the RG analysis during the pre-inflationary period is largely unaffected by the choice of the variant of the MSG model (see figures 7 and 8).

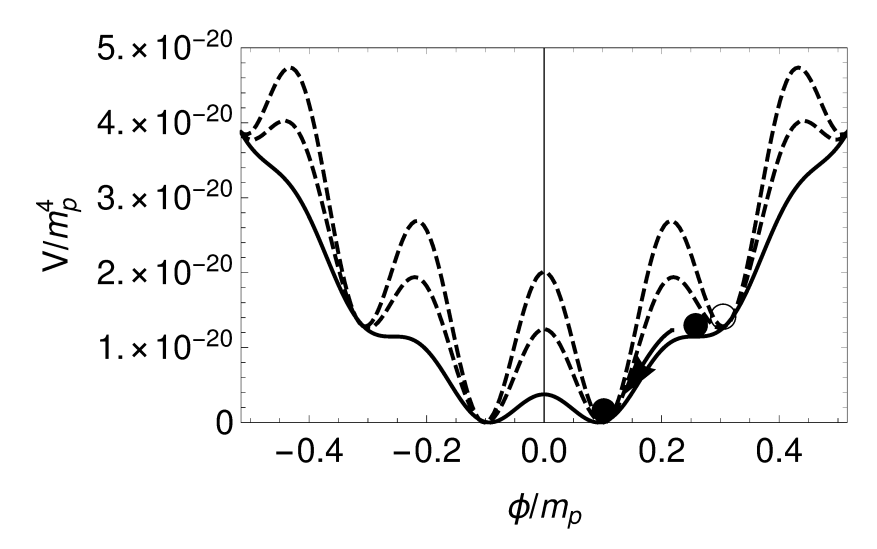


Figure 8. The same as figure 2, but for the third version of the MSG model (B.3). Here the normalized parameters, corresponding to the solid line, are $\hat{m} = 5.5 \times 10^{-10}$, $\hat{u} = 2.6 \times 10^{-21}$, $\hat{\beta} = 30$ which have been derived from the acceptance region of figure 5 using the slow-roll study with $\hat{\beta} = 30$. Just as in figure 7 (for the second version of the MSG model), and in contrast to the first variant of the MSG model (see figure 2), the third version of the MSG model predicts a nonvanishing vacuum expectation value of the inflaton field in the IR.

In order to have a prolonged exponential inflation with slow roll down [using reduced Planck units $c \equiv \hbar \equiv 1$ and $m_p^2 = 1/(8\pi G) \equiv 1$], the conditions given in eq. (3.15) must be fulfilled during inflation [4, 5]. Indeed, the inflation stops at ϕ_f if $\epsilon(\phi_{f,\epsilon})$ or $\eta(\phi_{f,\eta})$ reaches the value unity. Therefore, after substituting a potential, one can compute ϕ_f using the relation $\phi_f = \max{(\phi_{f,\epsilon}, \phi_{f,\eta})}$. The e-fold number N describes how many times the size of the Universe got larger by an e-fold and is defined in eq. (3.16); it is known to be in the range 50 < N < 60 (see refs. [11–13]). For example, using dimensionless quantities, the parameters ϵ , η and N can be expressed as follows for the first version of the MSG model,

$$\epsilon = \frac{1}{2} \left(\frac{\frac{\hat{u}}{\hat{m}^2} \hat{\beta} \sin(\hat{\beta}\hat{\phi}) + \hat{\phi}}{\frac{\hat{u}}{\hat{m}^2} \left[1 - \cos(\hat{\beta}\hat{\phi}) \right] + \frac{1}{2} \hat{\phi}^2} \right)^2, \tag{B.4}$$

$$\eta = \frac{\frac{\hat{u}}{\hat{m}^2} \hat{\beta}^2 \cos(\hat{\beta}\hat{\phi}) + 1}{\frac{\hat{u}}{\hat{m}^2} \left[1 - \cos(\hat{\beta}\hat{\phi}) \right] + \frac{1}{2}\hat{\phi}^2},$$
(B.5)

$$N = -\int_{\hat{\phi}_i}^{\hat{\phi}_f} d\hat{\phi} \frac{\frac{\hat{u}}{\hat{m}^2} \left[1 - \cos(\hat{\beta}\hat{\phi}) \right] + \frac{1}{2}\hat{\phi}^2}{\frac{\hat{u}}{\hat{\omega}^2} \hat{\beta} \sin(\hat{\beta}\hat{\phi}) + \hat{\phi}}.$$
 (B.6)

One finds similar results for the other two variants of the MSG model. These quantities only depend on the equally dimensionless ratio \hat{u}/\hat{m}^2 and the dimensionless frequency $\hat{\beta}$. If the mass term is negligible compared to the periodic one, then one obtains back the natural inflation (i.e., sine-Gordon) model. In the limit of a negligible periodic term (compared to the mass), one obtains the quadratic monomial inflationary model.

By choosing a particular value of N (e.g., N=55), the starting point of the inflation ϕ_i can be calculated using the integral (3.16) after substituting the previously obtained ϕ_f for a potential. Knowing ϕ_i , one can compute all relevant measurable quantities. These are

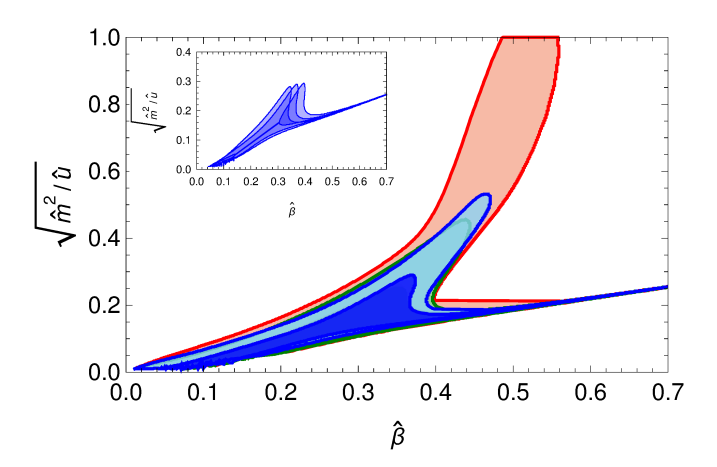


Figure 9. The same as figure 4, but for the second version of the MSG model (B.2). Regions of the parameter space of the second version of the MSG model (B.2) are indicated by different colors corresponding to different level of acceptance for N = 55, where the dark blue region gives the best fit to Planck data. The inset shows best acceptance regions for N = 50, 55, 60. For given data sets, dark color regions stand for 95% CL and the light-colored regions correspond to 68% CL.

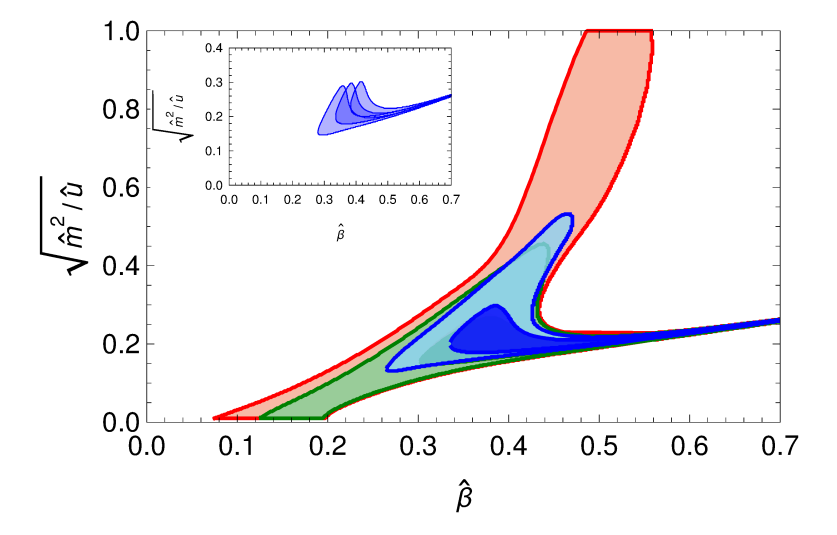


Figure 10. The same as figure 4 and figure 9, but for the third version of the MSG model (B.3).

the scalar tilt $n_s \approx 2 \eta(\phi_i) - 6 \epsilon(\phi_i) + 1$ and the tensor-to-scalar ratio $r \approx 6\epsilon(\phi_i)$. These quantities were measured by the PLANCK mission [11–13] and can be directly compared to theoretical calculations.

After performing the described calculations for different parameters of the first version of the MSG potential given in eq. (2.4), we obtain figures 3 and 4, where we indicate regions of the parameter space with different colors corresponding to different level of acceptance. The same slow-roll analysis has been performed for the last two versions of the MSG model [eqs. (B.2) and (B.3)] producing very similar results (see figures 9 and 10).

In order to fix not just the ratio \hat{u}/\hat{m}^2 and $\hat{\beta}$ but all three parameters of the potential, one must take into account the fact that the magnitude of the potential when the inflation started was $V(\phi_i) \equiv \frac{r}{0.01} (10^{16} \,\text{GeV})^4$. Therefore, the best dimensionful values for the two variants of the MSG model (2.4) and (B.2) taken from the slow-roll study read (see figure 9)

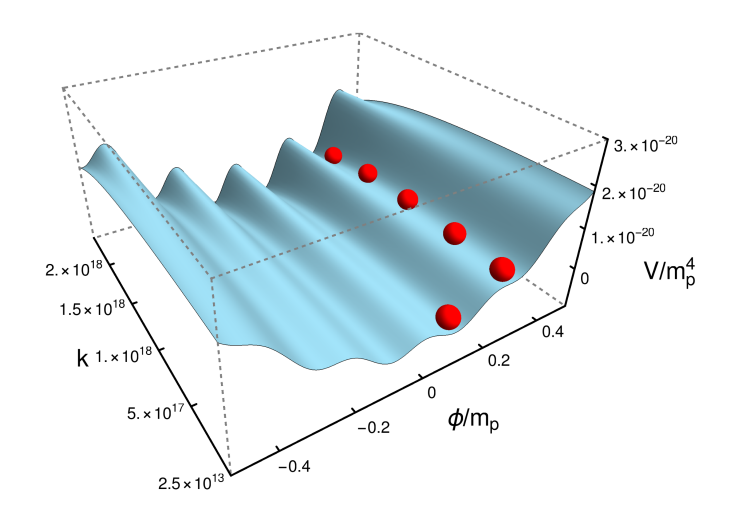


Figure 11. The same as figure 6 but for the variant (B.2) with $\hat{\beta} = 30$.

and figure 10) can be determined. For the MSG model (B.2), one finds

$$\frac{\hat{u}\hat{\beta}^2}{\hat{m}^2} = \frac{u_0 \beta_0^2}{m_0^2} \approx \frac{0.33^2}{0.17^2} > 1, \quad m_0 \approx 4.93 \times 10^{-6} m_p, \tag{B.7}$$

and thus $m_0 \approx 1.18 \times 10^{13} \, \text{GeV}$. For the model given in eq. (B.3), it reads as

$$\frac{\hat{u}\hat{\beta}^2}{\hat{m}^2} = \frac{u_0 \beta_0^2}{m_0^2} \approx \frac{0.39^2}{0.2^2} > 1, \quad m_0 \approx 4.89 \times 10^{-6} m_p \,, \tag{B.8}$$

where $m_0 \approx 1.176 \times 10^{13}$ GeV. Thus, the slow-roll study for small β provides parameters for the MSG model where the relation

$$\frac{u_0 \beta_0^2}{m_0^2} > 1 \tag{B.9}$$

always holds. The best parameters of eqs. (B.7) and (B.8) are very similar to each other in the small β region.

Let us discuss the change in the shape of the potentials (B.2) and (B.3) against the running RG scale k. This is visually represented in the 3D figures figure 11 and figure 12 [the corresponding 2D figures are figure 7 and figure 8].

Although in this work our focus is on the slow-roll study performed for small frequencies, it is important to discuss very briefly the limit of large $\hat{\beta}$. In particular, we would like to discuss how the constant (field-independent) term influences the best acceptance results, therefore we introduce the fourth version of the MSG model

$$V_{\text{MSG}_4}(\phi) = \frac{1}{2}m^2\phi^2 + u\cos(\beta\phi),$$
 (B.10)

which is obtained from eq. (2.4) by the replacement $u[1 - \cos(\beta\phi)] \to u \cos(\beta\phi)$. Let us consider the best acceptance regions for MSG type models where the periodic term has the same sign, i.e., for the models given in eqs. (B.2), (B.3) and (B.10). These regions overlap for large frequencies (see the straight (dark) line in figure 5). Thus, the addition constant term of (B.2), (B.3) and (B.10) do not play any role in the slow-roll study.

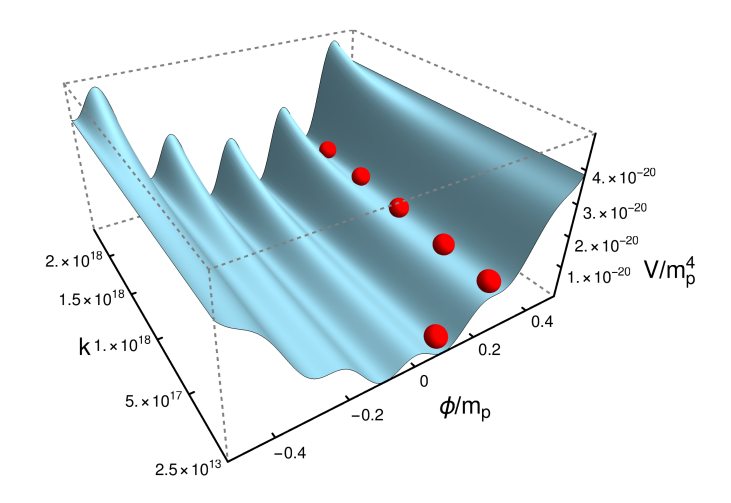


Figure 12. The same as figure 6 but for the variant (B.3) with $\hat{\beta} = 30$.

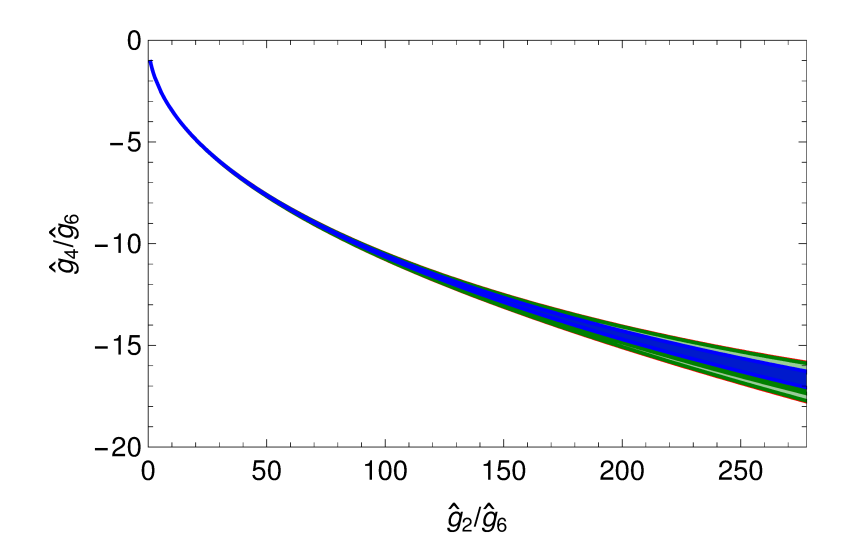


Figure 13. The same as figures 4, 9 and 10 given above, but for the ϕ^6 model (B.11). Regions of the parameter space are indicated by different colors corresponding to different level of acceptance for N=55, where the dark blue region gives the best fit to Planck data.

Finally, let us note that one of the conceivable interpretations of the MSG potential is that it is the UV completed potential of the Higgs, since the first two terms of its Taylor expansion recover the usual standard model which is bi-quadratic Higgs potential. Therefore, the ϕ field (in a more general model) can be a scalar doublet, but the potential depends only on the magnitude of this doublet and therefore, by a gauge transformation, it can be reduced to a single scalar field, as it is usually done when describing the Higgs (or, more accurately, the Brout-Englert-Higgs, or BEH) mechanism.

In conclusion, the theoretical predictions obtained from all types of MSG models are in an excellent agreement with observations in a well-defined region of parameter space, and therefore can be used to fix the parameters of the MSG models at the scale of inflation.

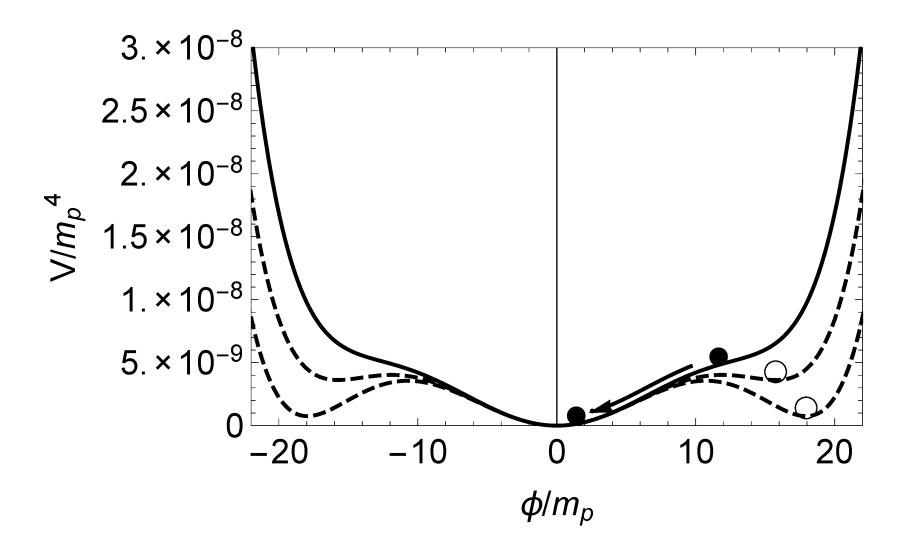


Figure 14. The shape of $V_{\phi^6} = \frac{1}{2}g_2\phi^2 + \frac{1}{4!}g_4\phi^4 + \frac{1}{6!}g_6\phi^6$ at various RG scales. The solid line stands for the potential at the scale of inflation $(k_i = 10^{16} \text{ GeV})$, determined from the acceptance region of figure 13 using the slow-roll study (see section B.2) with the choice $\hat{g}_2/\hat{g}_6 = 2/6! \times 10^5$. The resulting normalized parameters $(\hat{g}_2 = 1.4 \times 10^{-10}, \hat{g}_4 = -8.4 \times 10^{-12}, \hat{g}_6 = 5.0 \times 10^{-13})$ describe the potential over the whole inflationary period, where the VeV (full black circle) rolls down inducing inflation. The dashed lines correspond to UV values (pre-inflation), obtained considering known RG equations for the couplings of the ϕ^6 model, see e.g., ref. [82]. For further remarks on this point, see the discussion aroung eq. (B.15).

B.2 Slow-roll study of the ϕ^6 model

We also show the viability of our findings using the slow-roll analysis of the ϕ^6 model,

$$V_{\phi^6} = \frac{1}{2}g_2\phi^2 + \frac{1}{4!}g_4\phi^4 + \frac{1}{6!}g_6\phi^6,$$
 (B.11)

which is perturbatively nonrenormalizable but allows for UV extensions (in the sense of the MSG models) which are renormalizable by a nonperturbative RG, as discussed at length above. In the case of the ϕ^6 potential, the key quantities, ϵ, η and N, are described by the following expressions

$$\epsilon = \frac{1}{2} \left(\frac{\frac{\hat{g}_2}{\hat{g}_6} \hat{\phi} + \frac{1}{3!} \frac{\hat{g}_4}{\hat{g}_6} \hat{\phi}^3 + \frac{1}{5!} \hat{\phi}^5}{\frac{1}{2} \frac{\hat{g}_2}{\hat{g}_6} \hat{\phi}^2 + \frac{1}{4!} \frac{\hat{g}_4}{\hat{g}_6} \hat{\phi}^4 + \frac{1}{6!} \hat{\phi}^6} \right)^2, \tag{B.12}$$

$$\eta = \frac{\frac{\hat{g}_2}{\hat{g}_6} + \frac{1}{2}\frac{\hat{g}_4}{\hat{g}_6}\hat{\phi}^2 + \frac{1}{4!}\hat{\phi}^4}{\frac{1}{2}\frac{\hat{g}_2}{\hat{g}_6}\hat{\phi}^2 + \frac{1}{4!}\frac{\hat{g}_4}{\hat{g}_6}\hat{\phi}^4 + \frac{1}{6!}\hat{\phi}^6},$$
(B.13)

$$N = -\int_{\hat{\phi}_i}^{\hat{\phi}_f} d\hat{\phi} \frac{\frac{1}{2} \frac{\hat{g}_2}{\hat{g}_6} \hat{\phi}^2 + \frac{1}{4!} \frac{\hat{g}_4}{\hat{g}_6} \hat{\phi}^4 + \frac{1}{6!} \hat{\phi}^6}{\frac{\hat{g}_2}{\hat{g}_6} \hat{\phi} + \frac{1}{3!} \frac{\hat{g}_4}{\hat{g}_6} \hat{\phi}^3 + \frac{1}{5!} \hat{\phi}^5},$$
(B.14)

where the hat denotes dimensionless variables following the convention of eq. (3.13), i.e., $\hat{g}_2 = g_2/m_p^2$, $\hat{g}_4 = g_4$, $\hat{g}_6 = g_6 m_p^2$, $\hat{\phi} = \phi/m_p$. These, again, do not depend on the magnitude of the potential, but only on the ratios of the couplings \hat{g}_2/\hat{g}_6 and \hat{g}_4/\hat{g}_6 . In order to keep the potential to be bounded from below and have a false vacua one has to chose the signature $\hat{g}_2 > 0$, $\hat{g}_4 < 0$, $\hat{g}_6 > 0$ for the couplings.

A few remarks are in order, regarding the derivation of the RG equations that form the basis of figure 14. Namely, one might wonder how one could obtain RG equations for the ϕ^6 model when we have made the point in our paper that our main focus lies on the MSG model as the simplest nonperturbatively renormalizable UV completion of the ϕ^6 model, precisely for the reason that the ϕ^6 model is not perturbatively renormalizable in four dimensions. To this end, we should point out that the RG equations used by us should be taken with a grain of salt. Namely, they are obtained upon truncation of the Taylor expansion of eqs. (2.61) and (2.62) of ref. [82] in powers of ϕ , neglecting terms of order ϕ^8 , which would otherwise be generated by the RG flow. For completeness, we note the relevant RG equations used in figure 14,

$$k\partial_k \tilde{g}_2 = -2\tilde{g}_2 - \frac{\tilde{g}_4}{32\pi^2(1+\tilde{g}_2)^2},$$
 (B.15a)

$$k\partial_k \tilde{g}_4 = -\frac{\tilde{g}_2 \tilde{g}_6 - 6\tilde{g}_4^2 + \tilde{g}_6}{32\pi^2 (1 + \tilde{g}_2)^3},$$
(B.15b)

$$k\partial_k \tilde{g}_6 = 2\tilde{g}_6 + \frac{15\tilde{g}_4 \left(\tilde{g}_2 \tilde{g}_6 - 3\tilde{g}_4^2 + \tilde{g}_6\right)}{16\pi^2 (1 + \tilde{g}_2)^4} \,. \tag{B.15c}$$

After performing the RG, as shown in figure 14, using the same method described in the previous section, performing the slow-roll analysis, one obtains figure 13. This shows, given the fact that PLANCK data are sensitive only to the slow-roll of the potential (near the end of inflation), that the ϕ^6 model can describe the observations made by the PLANCK mission. However, due to its nonrenormalizability, it cannot serve as a viable UV completion of the inflaton potential.

C Convexity and RG running

Finally, let us discuss the connection between the convexity and the RG running of the effective action. The functional RG method is a possible choice to determine the RG running of the parameters. In some sense, the functional RG equation interpolates between the classical (bare) and the quantum effective action. The initial condition for the RG equation is usually known and its determination is based on symmetry considerations. The RG method is used to obtain the low energy (IR) effective theory of a model given at the high energy (UV) momentum cutoff. However, in this work we have to follow a different strategy. We select between various possible inflationary potentials by performing their slow-roll study which fixes their parameters and the scale of inflation serves as an IR value for the RG running. Thus, as a first step, one has to explore possible UV completions of the models defined by the slow-roll study at low energies. In some sense, we here attempt to provide a "mini crash course" in the functional RG suited to the problem at hand.

In order to apply the method of RG running induced inflation, the UV completed potential has to have a false vacuum which requires, in a power series ansatz, at least a term of order ϕ^6 . Moreover, in d=4 dimensions, terms of ϕ^6 and higher powers of the field are nonrenormalizable perturbatively. They generates under RG flow, higher order terms (i.e., monomials of arbitrarily high order). This suggests an UV-completion of the model with a functional form that involves a non-terminating power series in ϕ . These models eo ipso require a non-perturbative RG analysis which can be done by the use of the Wetterich RG

equation [64, 65],

$$k\partial_k \Gamma_k = \frac{\hbar}{2} \int \frac{d^d p}{(2\pi)^d} \frac{k\partial_k R_k}{R_k + \Gamma_k^{(2)}},\tag{C.1}$$

derived for the one-component scalar field theory [64, 65]. Let us first discuss its connection to the effective action which has the following form at the 1-loop level,

$$\Gamma_{\text{eff}} = S_{\Lambda} + \frac{\hbar}{2} \int \frac{d^d p}{(2\pi)^d} \ln \left[S_{\Lambda}^{(2)} \right] + \mathcal{O}(\hbar^2), \tag{C.2}$$

where S_{Λ} is the classical (bare) action. The momentum integral can be divergent at its upper (UV) and lower (IR) bounds. A momentum cutoff is a standard choice to regularize the integral; however, one can choose a Pauli-Villars approach by adding a momentum dependent mass term $\frac{1}{2} \int R_k(p) \phi^2$ to the bare (classical) action, and introduce a scale-dependent action

$$\Gamma_k \equiv S_{\Lambda} + \frac{\hbar}{2} \int \frac{d^d p}{(2\pi)^d} \ln \left[R_k + S_{\Lambda}^{(2)} \right] , \qquad (C.3)$$

which recovers the classical and the effective action (at 1-loop) in the UV and IR limits if the regulator function $R_k(p)$ fulfills the following requirements [see eqs. (13)—(15) of ref. [81]]

$$R_{k\to 0}(p) = 0, \tag{C.4a}$$

$$R_{k\to\Lambda}(p) = \infty$$
, (C.4b)

$$R_k(p \to 0) > 0. \tag{C.4c}$$

In a nutshell, the first of these conditions implies that one recovers the effective action in the limit $k \to 0$, the second ensures that the bare action is recovered for $k \to \Lambda$ (within the limitations explained in the following), and the third ensures that the regulator implements an IR regularization.

The divergence of the regulator for $k \to \Lambda$, though, implies that Γ_k only recovers the bare action at $k = \Lambda$ up to a field-independent, but k-dependent, term. This is also the reason why, in eq. (10) of ref. [81], as well in the text between eqs. (15) and (16) of ref. [81], one writes

$$\Gamma_{k\to 0} = \Gamma_{\text{eff}} \,, \tag{C.5}$$

$$\Gamma_{k \to \Lambda} = \Gamma_{\Lambda} = S_{\Lambda} + \text{const.} \simeq S_{\Lambda}.$$
 (C.6)

The latter identification may be part of the reason for the known fact (see section 2.3 of ref. [81]) that the formulation of the RG evolution of the constant, field-independent term requires special care within the nonperturbative approach implied by the Wetterich equation. Moreover, eq. (C.4b) [when inserted into eq. (C.3)] implies that the "constant term" in eq. (C.6) actually is given by a divergent integral. Let us note that the last requirement for the regulator in (C.4a) is necessary to remove IR divergences in the momentum integral. As a second step one can differentiate eq. (C.3) with respect to the running scale k

$$\partial_k \Gamma_k = \frac{\hbar}{2} \int \frac{d^d p}{(2\pi)^d} \frac{\partial_k R_k}{R_k + S_{\Lambda}^{(2)}}.$$
 (C.7)

Finally, in order to have an exact (1-loop improved) expression, the bare action at the right hand side should be replaced by the scale-dependent one, i.e., $S_{\Lambda}^{(2)} \to \Gamma_k^{(2)}$ (and both sides multiplied by k) which results in the "exact" functional RG equation (C.1).

Now, let us show why the effective potential should be convex [85]. The effective action is the Legendre transformation of W[J], which is the generating functional for the connected Green-functions

$$\Gamma_{\text{eff}}[\phi] = -W[J] + \int J\phi. \tag{C.8}$$

If one fixes the field and the source to constant values $(\phi(x) = \phi_0, J(x) = J_0)$ in the spacetime volume Ω , then the effective action reduces to the effective potential as follows

$$\Gamma_{\text{eff}}[\phi] = \Omega V_{\text{eff}}(\phi_0), \quad W[J] = \Omega w(J_0).$$
 (C.9)

Using the relations of the Legendre transformation for the reduced functions

$$\phi_0 = \frac{\delta w[J_0]}{\delta J_0}, \quad J_0 = \frac{\delta V_{\text{eff}}[\phi_0]}{\delta \phi_0}, \tag{C.10}$$

one obtains the following equation by differentiating the effective potential with respect to the field and the source by using the chain rule,

$$\left(\frac{\delta^2 V_{\text{eff}}}{\delta \phi_0 \delta \phi_0}\right) \left(\frac{\delta^2 w}{\delta J_0 \delta J_0}\right) = 1.$$
(C.11)

The second derivative of the generating functional of the connected Green functions with respect to the source term is the connected correlation function which should be positive. Thus, the convexity of the effective action comes from eq. (C.11)

$$\left(\frac{\delta^2 V_{\text{eff}}}{\delta \phi_0 \delta \phi_0}\right) \ge 0.$$
(C.12)

On one hand, the non-perturbative RG equation (C.1) should recover the full quantum effective action in the IR $(k \to 0)$ limit. On the other hand, we have just shown that the effective action or more precisely the effective potential should be convex. Therefore, if one performs the RG study of a possible UV-completion of the ϕ^6 model (B.11), the false vacua start to vanish under the RG flow creating first a flat region of the potential, ideal for the slow-roll, see figure 14, which is the cornerstone of the RG running induced inflation method proposed in this work.

D RG evolution of the constant term

A relatively subtle problem should be mentioned. Namely, from eq. (3.1), one could in principle derive an RG equation for the constant term $V_k(\phi = 0)$. (Re-)written for the dimensionful potential, the (naively obtained) RG equation for $V_k(0)$ reads as follows (d = 4),

$$k\partial_k V_k(0) = \frac{k^4}{32\pi^2} \frac{k^2}{k^2 + \partial_\phi^2 V_k(0)}.$$
 (D.1)

In the limit $k^2 \gg \partial_\phi^2 V(0)$, the solution to eq. (D.1) is

$$V_k(0) = V_{\Lambda}(0) + \frac{k^4 - \Lambda^4}{128\pi^2},$$
(D.2)

which would otherwise indicate a rampant quartic divergence of $V_k(0)$ in the limit of large Λ , and lead to a considerable change in $V_k(0)$ between the Planck and the GUT scales, possibly requiring fine-tuning of the model in the UV limit, i.e., at the Planck scale. The problem is important since $V_k(0)$ is associated with the cosmological constant term.

In order to fully address the problem, it is necessary to include a longer discussion. We first observe that the functional form of the potential given in eq. (2.4) implies that $V_k(0) = 0$ irrespective of the numerical values of m, u, and β , while the full potential vanishes for any field only if m = 0 and u = 0. The nonperturbative RG running of the potential could still imply the possibility of a k-dependence of $V_k(0)$, which, in the large-k limit, could be deemed to be described by eq. (D.2), in which case it becomes independent of the numerical values of m, u, and β . The latter observation is consistent with the general argument presented below, which implies that the rampant k^4 behavior is due to the emergence of the spurious terms from the UV properties of the regulator used in the formulation of the nonperturbative RG equation [see eq. (15) of ref. [81]]. Indeed, the limit of a vanishing potential $(u \to 0, m \to 0)$ must be approached smoothly, and subtractions to the RG equation (D.1) are required.

As suggested by the quantum mechanical calculation [see eq. (37) of ref. [81]], one is led to the following subtraction

$$\frac{k^2}{k^2 + \partial_{\phi}^2 V_k(0)} \to \frac{k^2}{k^2 + \partial_{\phi}^2 V_k(0)} - 1, \qquad (D.3)$$

which reduces the divergence of the RG evolution in the UV and alleviates the fine-tuning problem in the UV. Subtractions similar to eq. (D.3) are well known to produce correct results for the free energy in quantum-mechanical models, and in statistical mechanics. In the present case, this would correspond to the free energy of the inflaton field in the flat background limit.

Subtraction schemes different from equation (D.3) can be proposed [86]. Yet, a deeper analysis of the RG running of field-independent constant terms, and their extension for non-flat backgrounds is beyond the scope of the present paper. An investigation of the conditions that could fix, at least partially, the subtraction scheme is currently in progress, and will be reported elsewhere [86]. In particular, a decisive question under investigation is whether or not the generation of the unphysical divergences for the constant, field-independent terms could be avoided via a modification of the conditions imposed on the regulator function (C.4).

References

- [1] A.H. Guth, The inflationary universe: a possible solution to the horizon and flatness problems, Phys. Rev. **D 23** (1981) 347 [INSPIRE].
- [2] A.A. Starobinsky, A new type of isotropic cosmological models without singularity, Phys. Lett. 91B (1980) 99 [INSPIRE].
- [3] V.F. Mukhanov and G.V. Chibisov, Quantum fluctuations and a nonsingular universe, JETP Lett. 33 (1981) 532 [Pisma Zh. Eksp. Teor. Fiz. 33 (1981) 549] [INSPIRE].
- [4] A.D. Linde, A new inflationary universe scenario: a possible solution of the horizon, flatness, homogeneity, isotropy and primordial monopole problems, Phys. Lett. 108B (1982) 389 [INSPIRE].
- [5] A. Albrecht and P.J. Steinhardt, Cosmology for Grand Unified Theories with radiatively induced symmetry breaking, Phys. Rev. Lett. 48 (1982) 1220 [INSPIRE].

- [6] J. Martin, C. Ringeval and V. Vennin, Encyclopaedia inflationaris, Phys. Dark Univ. 5-6 (2014) 75.
- [7] A. Friedmann, Über die Krümmung des Raumes, Z. Phys. A 10 (1922) 377.
- [8] G. Lemaître, A homogeneous universe of constant mass and increasing radius accounting for the radial velocity of extra-galactic nebulae, Mon. Not. Roy. Astron. Soc. **91** (1931) 483.
- [9] H.P. Robertson, Kinematics and world-structure, Astrophys. J. 82 (1935) 284 [INSPIRE].
- [10] A.G. Walker, On Milne's theory of world-structure, Proc. London Math. Soc. 42 (1937) 90.
- [11] Planck collaboration, Planck 2015 results. XIII. Cosmological parameters, Astron. Astrophys. 594 (2016) A13 [arXiv:1502.01589].
- [12] Planck collaboration, Planck 2015 results. XX. Constraints on inflation, Astron. Astrophys. 594 (2016) A20 [arXiv:1502.02114].
- [13] BICEP2, Keck Array collaboration, Improved constraints on cosmology and foregrounds from BICEP2 and Keck Array Cosmic Microwave Background data with inclusion of 95 GHz band, Phys. Rev. Lett. 116 (2016) 031302 [arXiv:1510.09217] [INSPIRE].
- [14] M. Iihoshi, Mutated hybrid inflation in $f(R, \Box R)$ -gravity, JCAP **02** (2011) 022 [arXiv:1011.3927] [INSPIRE].
- [15] J. Earman and J. Mosterin, A critical look at inflationary cosmology, Phil. Sci. 66 (1999) 1.
- [16] P.J. Steinhardt, The inflation debate, Scient. Amer. 304 (2011) 36.
- [17] J. Rubio, Higgs inflation, Front. Astron. Space Sci. 5 (2019) 50.
- [18] A. Bonanno and M. Reuter, Cosmology of the Planck era from a renormalization group for quantum gravity, Phys. Rev. D 65 (2002) 043508 [hep-th/0106133] [INSPIRE].
- [19] A. Bonanno and M. Reuter, Cosmology with selfadjusting vacuum energy density from a renormalization group fixed point, Phys. Lett. B 527 (2002) 9 [astro-ph/0106468] [INSPIRE].
- [20] A. Bonanno and M. Reuter, Cosmological perturbations in renormalization group derived cosmologies, Int. J. Mod. Phys. D 13 (2004) 107 [astro-ph/0210472] [INSPIRE].
- [21] E. Bentivegna, A. Bonanno and M. Reuter, Confronting the IR fixed point cosmology with high-redshift observations, JCAP 01 (2004) 001 [astro-ph/0303150].
- [22] I.L. Shapiro and J. Solà, Scaling behavior of the cosmological constant: Interface between quantum field theory and cosmology, JHEP 02 (2002) 006 [hep-th/0012227] [INSPIRE].
- [23] I.L. Shapiro and J. Solà, Massive fields temper anomaly induced inflation, Phys. Lett. B 530 (2002) 10 [hep-ph/0104182] [INSPIRE].
- [24] I.L. Shapiro and J. Solà, On the scaling behavior of the cosmological constant and the possible existence of new forces and new light degrees of freedom, Phys. Lett. B 475 (2000) 236 [hep-ph/9910462] [INSPIRE].
- [25] I.L. Shapiro and J. Solà, Cosmological constant, renormalization group and Planck scale physics, Nucl. Phys. Proc. Suppl. 127 (2004) 71 [hep-ph/0305279] [INSPIRE].
- [26] L. Shapiro, J. Sola and H. Stefancic, Running G and Λ at low energies from physics at M_X : possible cosmological and astrophysical implications, JCAP 01 (2005) 012 [hep-ph/0410095].
- [27] I.L. Shapiro and J. Solà, On the possible running of the cosmological 'constant', Phys. Lett. B 682 (2009) 105 [arXiv:0910.4925] [INSPIRE].
- [28] Y.-F. Cai et al., Planck constraints on Higgs modulated reheating of renormalization group improved inflation, Phys. Rev. D 88 (2013) 083508 [arXiv:1304.6938] [INSPIRE].
- [29] G. Kofinas and V. Zarikas, Asymptotically safe gravity and non-singular inflationary Big Bang with vacuum birth, Phys. Rev. **D** 94 (2016) 103514 [arXiv:1605.02241] [INSPIRE].

- [30] R. Moti and A. Shojai, On the effect of renormalization group improvement on the cosmological power spectrum, Eur. Phys. J. C 78 (2018) 32 [arXiv:1703.02733] [INSPIRE].
- [31] A. Kaya, Exact renormalization group flow in an expanding Universe and screening of the cosmological constant, Phys. Rev. D 87 (2013) 123501 [arXiv:1303.5459] [INSPIRE].
- [32] J. Serreau, Renormalization group flow and symmetry restoration in de Sitter space, Phys. Lett.
 B 730 (2014) 271 [arXiv:1306.3846].
- [33] T. Prokopec and G. Rigopoulos, Functional renormalization group for stochastic inflation, JCAP 08 (2018) 013 [arXiv:1710.07333].
- [34] M. Guilleux and J. Serreau, Quantum scalar fields in de Sitter space from the nonperturbative renormalization group, Phys. Rev. D 92 (2015) 084010 [arXiv:1506.06183] [INSPIRE].
- [35] B. Guberina, R. Horvat and H. Stefancic, Renormalization group running of the cosmological constant and the fate of the universe, Phys. Rev. **D** 67 (2003) 083001 [hep-ph/0211184] [INSPIRE].
- [36] M. Reuter and H. Weyer, Renormalization group improved gravitational actions: a Brans-Dicke approach, Phys. Rev. **D** 69 (2004) 104022 [hep-th/0311196] [INSPIRE].
- [37] M. Reuter and H. Weyer, Running Newton constant, improved gravitational actions and galaxy rotation curves, Phys. Rev. D 70 (2004) 124028 [hep-th/0410117] [INSPIRE].
- [38] A. Babic, B. Guberina, R. Horvat and H. Stefancic, Renormalization-group running cosmologies. A scale-setting procedure, Phys. Rev. D 71 (2005) 124041 [astro-ph/0407572] [INSPIRE].
- [39] A. Bonanno and M. Reuter, Spacetime structure of an evaporating black hole in quantum gravity, Phys. Rev. D 73 (2006) 083005 [hep-th/0602159] [INSPIRE].
- [40] D. Lopez Nacir and F.D. Mazzitelli, Running of Newton's constant and non integer powers of the d'Alembertian, Phys. Rev. D 75 (2007) 024003 [hep-th/0610031] [INSPIRE].
- [41] A. Contillo, Evolution of cosmological perturbations in an RG-driven inflationary scenario, Phys. Rev. D 83 (2011) 085016 [arXiv:1011.4618] [INSPIRE].
- [42] A. Contillo, M. Hindmarsh and C. Rahmede, Renormalisation group improvement of scalar field inflation, Phys. Rev. **D** 85 (2012) 043501 [arXiv:1108.0422] [INSPIRE].
- [43] M. Hindmarsh and I.D. Saltas, f(R) gravity from the renormalisation group, Phys. Rev. **D** 86 (2012) 064029 [arXiv:1203.3957] [INSPIRE].
- [44] E.J. Copeland, C. Rahmede and I.D. Saltas, Asymptotically safe Starobinsky inflation, Phys. Rev. D 91 (2015) 103530 [arXiv:1311.0881] [INSPIRE].
- [45] G. D'Odorico and F. Saueressig, Quantum phase transitions in the Belinsky-Khalatnikov-Lifshitz universe, Phys. Rev. **D 92** (2015) 124068 [arXiv:1511.00247] [INSPIRE].
- [46] G. Kofinas and V. Zarikas, Solution of the dark energy and its coincidence problem based on local antigravity sources without fine-tuning or new scales, Phys. Rev. **D** 97 (2018) 123542 [arXiv:1706.08779] [INSPIRE].
- [47] I.L. Shapiro, J. Solà, C. Espana-Bonet and P. Ruiz-Lapuente, Variable cosmological constant as a Planck scale effect, Phys. Lett. B 574 (2003) 149 [astro-ph/0303306] [INSPIRE].
- [48] C. Espana-Bonet, P. Ruiz-Lapuente, I.L. Shapiro and J. Sola, Testing the running of the cosmological constant with Type Ia supernovae at high z, JCAP 02 (2004) 006 [hep-ph/0311171].
- [49] I.L. Shapiro and J. Solà, A Friedmann-Lemaitre-Robertson-Walker cosmological model with running Lambda, astro-ph/0401015 [INSPIRE].

- [50] J. Solà, Dark energy: a quantum fossil from the inflationary Universe?, J. Phys. A 41 (2008) 164066 [arXiv:0710.4151] [INSPIRE].
- [51] J. Solà, A. Gómez-Valent and J. de Cruz Pérez, First evidence of running cosmic vacuum: challenging the concordance model, Astrophys. J. 836 (2017) 43 [arXiv:1602.02103] [INSPIRE].
- [52] S. Basilakos, N. E. Mavromatos and J. Sola Paracaula, Quantum anomalies in string-inspired running vacuum universe: inflation and axion dark matter, Phys. Lett. B 803 (2020) 135342.
- [53] J. Solà and A. Gómez-Valent, The $\bar{\Lambda}$ CDM cosmology: from inflation to dark energy through running Λ , Int. J. Mod. Phys. **D 24** (2015) 1541003 [arXiv:1501.03832] [INSPIRE].
- [54] S. Basilakos, N.E. Mavromatos and J. Solà Peracaula, Gravitational and chiral anomalies in the running vacuum universe and matter-antimatter asymmetry, Phys. Rev. **D** 101 (2020) 045001 [arXiv:1907.04890] [INSPIRE].
- [55] L.P. Kadanoff, Scaling laws for ising models near T_c, Physics 2 (1966) 263.
- [56] K.G. Wilson, Model Hamiltonians for Local Quantum Field Theory, Phys. Rev. 140 (1965) B445 [INSPIRE].
- [57] J. Polonyi, Lectures on the functional renormalization group method, Cent. Eur. J. Phys. 1 (2003) 1.
- [58] D. Baumann, Inflation, arXiv:0907.5424 [INSPIRE].
- [59] K. Freese, J.A. Frieman and A.V. Olinto, Natural inflation with pseudo Nambu-Goldstone bosons, Phys. Rev. Lett. 65 (1990) 3233 [INSPIRE].
- [60] K. Freese and W.H. Kinney, Natural inflation: consistency with cosmic microwave background observations of Planck and BICEP2, JCAP 03 (2015) 044 [arXiv:1403.5277].
- [61] P. Creminelli et al., ϕ^2 or not ϕ^2 : testing the simplest inflationary potential, Phys. Rev. Lett. 112 (2014) 241303 [arXiv:1404.1065] [INSPIRE].
- [62] T. Kobayashi, O. Seto and Y. Yamaguchi, Axion monodromy inflation with sinusoidal corrections, Prog. Theor. Exp. Phys. 2014 (2014) 103E01 [arXiv:1404.5518].
- [63] T. Higaki, T. Kobayashi, O. Seto and Y. Yamaguchi, Axion monodromy inflation with multi-natural modulations, JCAP 10 (2014) 025 [arXiv:1405.0775].
- [64] C. Wetterich, Exact evolution equation for the effective potential, Phys. Lett. B 301 (1993) 90 [arXiv:1710.05815] [INSPIRE].
- [65] T.R. Morris, The exact renormalization group and approximate solutions, Int. J. Mod. Phys. A 9 (1994) 2411 [hep-ph/9308265] [INSPIRE].
- [66] L.V. Keldysh, Diagram technique for nonequilibrium processes, Zh. Eksp. Teor. Fiz. 47 (1964) 1515 [Sov. Phys. JETP 20 (1965) 1018] [INSPIRE].
- [67] O.V. Konstantinov and V.I. Perel, A graphical technique for computation of kinetic quantities, Zh. Eksp. Teor. Fiz. 39 (1960) 197 [Sov. Phys. JETP 12 (1961) 142].
- [68] J.S. Schwinger, Brownian motion of a quantum oscillator, J. Math. Phys. 2 (1961) 407 [INSPIRE].
- [69] L.P. Kadanoff and G. Baym, *Quantum statistical mechanics*, Benjamin, New York U.S.A. (1962).
- [70] J. Polonyi, Quantum-classical crossover in electrodynamics, Phys. Rev. D 74 (2006) 065014 [hep-th/0605218] [INSPIRE].
- [71] S. Nagy, J. Polonyi and I. Steib, Quantum renormalization group, Phys. Rev. **D** 93 (2016) 025008 [arXiv:1508.04277] [INSPIRE].

- [72] S. Nagy, J. Polonyi and I. Steib, Euclidean scalar field theory in the bilocal approximation, Phys. Rev. D 97 (2018) 085002 [arXiv:1801.08171] [INSPIRE].
- [73] R. Brustein, S.P. de Alwis and P. Martens, Cosmological stabilization of moduli with steep potentials, Phys. Rev. D 70 (2004) 126012 [hep-th/0408160] [INSPIRE].
- [74] A. Codello, N. Defenu and G. D'Odorico, Critical exponents of O(N) models in fractional dimensions, Phys. Rev. **D** 91 (2015) 105003 [arXiv:1410.3308] [INSPIRE].
- [75] N. Defenu and A. Codello, Scaling solutions in the derivative expansion, Phys. Rev. **D** 98 (2018) 016013 [arXiv:1711.01809] [INSPIRE].
- [76] D.F. Litim, Optimization of the exact renormalization group, Phys. Lett. B 486 (2000) 92 [hep-th/0005245] [INSPIRE].
- [77] I. Nandori, S. Nagy, K. Sailer and A. Trombettoni, Comparison of renormalization group schemes for sine-Gordon type models, Phys. Rev. **D** 80 (2009) 025008 [arXiv:0903.5524] [INSPIRE].
- [78] I. Nandori, On the renormalization of the bosonized multi-flavor Schwinger model, Phys. Lett. **B** 662 (2008) 302 [arXiv:0707.2745] [INSPIRE].
- [79] S. Nagy, I. Nandori, J. Polonyi and K. Sailer, Generalized universality in the massive sine-Gordon model, Phys. Rev. D 77 (2008) 025026 [hep-th/0611216] [INSPIRE].
- [80] I. Nandori, Bosonization and functional renormalization group approach in the framework of QED₂, Phys. Rev. D 84 (2011) 065024 [arXiv:1008.2934] [INSPIRE].
- [81] H. Gies, Introduction to the functional RG and applications to gauge theories, Lect. Notes Phys. 852 (2012) 287 [hep-ph/0611146] [INSPIRE].
- [82] B. Delamotte, An introduction to the nonperturbative renormalization group, Lect. Notes Phys. 852 (2012) 49 [cond-mat/0702365].
- [83] D.H. Lyth, Particle physics models of inflation, Lect. Notes Phys. 738 (2008) 81 [hep-th/0702128] [INSPIRE].
- [84] D.H. Lyth and A. Riotto, Particle physics models of inflation and the cosmological density perturbation, Phys. Rept. **314** (1999) 1 [hep-ph/9807278] [INSPIRE].
- [85] R.J. Rivers, *Path integral methods in quantum field theory*, Cambridge University Press, Cambridge U.K. (1987).
- [86] U.D. Jentschura et al., Role of field-independent terms in nonperturbative RG, in preparation.